

Model-Based Deep Learning

Nir Shlezinger, Jay Whang, Yonina C. Eldar, and Alexandros G. Dimakis

Abstract—Signal processing, communications, and control have traditionally relied on classical statistical modeling techniques. Such model-based methods utilize mathematical formulations that represent the underlying physics, prior information and additional domain knowledge. Simple classical models are useful but sensitive to inaccuracies and may lead to poor performance when real systems display complex or dynamic behavior.

On the other hand, purely data-driven approaches that are model-agnostic are becoming increasingly popular as datasets become abundant and the power of modern deep learning pipelines increases. Deep neural networks (DNNs) use generic architectures which learn to operate from data, and demonstrate excellent performance, especially for supervised problems. However, DNNs typically require massive amounts of data and immense computational resources, limiting their applicability for some signal processing scenarios.

We are interested in hybrid techniques that combine principled mathematical models with data-driven systems to benefit from the advantages of both approaches. Such model-based deep learning methods exploit both partial domain knowledge, via mathematical structures designed for specific problems, as well as learning from limited data. In this article we survey the leading approaches for studying and designing model-based deep learning systems. We divide hybrid model-based/data-driven systems into categories based on their inference mechanism. We provide a comprehensive review of the leading approaches for combining model-based algorithms with deep learning in a systematic manner, along with concrete guidelines and detailed signal processing oriented examples from recent literature. Our aim is to facilitate the design and study of future systems on the intersection of signal processing and machine learning that incorporate the advantages of both domains.

I. INTRODUCTION

Traditional signal processing is dominated by algorithms that are based on simple mathematical models which are hand-designed from domain knowledge. Such knowledge can come from postulated simple statistical models, or from fixed deterministic models which represent the particular problem at hand. These domain-knowledge-based processing algorithms, which we refer to henceforth as *model-based methods*, carry out inference based on knowledge of the underlying model relating the observations at hand and the desired information. Model-based methods do not rely on data to learn their mapping, though data is often used to estimate a small number of parameters. Fundamental techniques like the Kalman filter and message passing algorithms belong to the class of model-based methods. Classical statistical models rely on simplifying assumptions (e.g. linear systems, Gaussian and independent noise, etc.) that make models tractable, understandable and

computationally efficient. On the other hand, simple models frequently fail to represent nuances of high-dimensional complex data and dynamic variations.

The incredible success of deep learning e.g., on vision [1], [2] as well as challenging games such as Go [3] and Starcraft [4], has initiated a general data-driven mindset. It is currently fashionable to replace simple principled models with purely data-driven pipelines, trained with massive labeled datasets. Deep neural networks (DNNs) can be trained in a supervised way end-to-end to map inputs to predictions. The benefits of data-driven methods over model-based approaches are twofold: First, purely-data-driven methods do not rely on analytical approximations and thus can operate in scenarios where analytical models are not known. Second, for complex systems, data-driven methods are able to extract semantic information from observed data [5]. This is sometimes difficult to achieve analytically, even when complex models are perfectly known.

The fact that massive data sets are typically required to train highly-parametrized DNNs to learn a desirable mapping, and the computational burden of training and utilizing these networks, may constitute a major drawback in various signal processing, communications, and control applications. For example, consider the simplistic communication setup illustrated in Fig. 1, where two receivers recover the transmitted messages based on their observations, using model-based algorithms and model-agnostic DNNs, respectively. The dynamic nature of wireless channels implies that the receivers must track channel variations in order to continue to reliably detect the transmitted messages over long periods of time. To do so, the model-based receiver in Fig. 1(a) can periodically estimate the model parameters imposed on the underlying statistics, a task which is known to be feasible under conventional channel models using periodic pilots embedded in communication standards. For the same purpose, the DNN-based receiver in Fig. 1(b) needs to periodically re-train its DNN to track channel variations. The fact that doing so requires a large data set is directly translated to a massive overhead decreasing the spectral efficiency, which adds to the considerable computational effort required for training. Furthermore, the high computational burden associated with highly-parametrized DNNs severely limits their applicability on hardware-limited devices, such as mobile phones, unmanned aerial vehicles, and Internet of Things (IOT) systems [6]. Finally, DNNs are commonly utilized as black-boxes; understanding how their predictions are obtained and characterizing confidence intervals tends to be quite challenging. As a result, deep learning does not yet offer the interpretability, flexibility, versatility, and reliability of model-based methods [7].

The limitations associated with model-based methods and black-box deep learning systems gave rise to a multitude

N. Shlezinger is with the School of ECE, Ben-Gurion University of the Negev, Be'er-Sheva, Israel (e-mail: nirshl@bgu.ac.il). J. Whang is with the Department of CS, University of Texas at Austin, Austin, TX (e-mail: jaywhang@cs.utexas.edu). Y. C. Eldar is with the Faculty of Math and CS, Weizmann Institute of Science, Rehovot, Israel (e-mail: yonina@weizmann.ac.il). A. G. Dimakis is with the Department of ECE, University of Texas at Austin, Austin, TX (e-mail: dimakis@austin.utexas.edu).

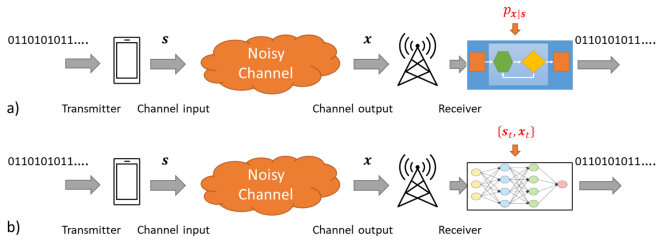


Fig. 1: Model-based methods versus deep learning for symbol detection: a) a receiver uses its knowledge of the statistical channel, denoted $p_{x|s}$ to detect the transmitted symbols in a model-based manner; b) a receiver utilizes a DNN trained using the data set $\{s_t, x_t\}$ for recovering the symbols.

of techniques for combining signal processing and machine learning to benefit from both approaches. These methods are application-driven, and are thus designed and studied in light of a specific task. For example, the combination of DNNs and model-based compressed sensing (CS) recovery algorithms was shown to facilitate sparse recovery [8], [9] as well as enable CS beyond the domain of sparse signals [10]–[12]; Deep learning was used to empower regularized optimization methods [13], [14], while model-based optimization contributed to the design of DNNs for such tasks [15]; Digital communication receivers used DNNs to learn to carry out symbol detection algorithms in a data-driven manner [16]–[18], while symbol recovery methods enabled the design of model-aware deep receivers [19], [20]. The proliferation of hybrid model-based/data-driven systems, each designed for a unique task, motivates establishing a concrete systematic framework for combining domain knowledge in the form of model-based methods and deep learning, which is the focus of this article.

In this article we present the leading strategies for combining domain knowledge and data via model-based deep learning in a tutorial fashion. To that aim, we present a unified framework for studying and designing hybrid model-based/data-driven systems, without focusing on a specific application, while being geared towards families of problems typically studied in the signal processing literature. The proposed framework builds upon the insight that, regardless of their specific task, systems combining model-based signal processing and deep learning can be divided based on the component which eventually infers: The first category are DNNs whose architecture is specialized to the specific problem using model-based methods, referred to here as *model-aided networks*. The second one are techniques in which inference is carried out by a model-based algorithm whose operation is empowered by deep learning, which we refer to as *DNN-aided inference*. Based on this division, we provide concrete guidelines for studying, designing, and comparing model-based deep learning systems. An illustration of the proposed division of model-based deep learning schemes into categories and sub-categories is depicted in Fig. 2.

We begin by discussing the high level concepts of model-based, data-driven, and hybrid schemes. Since we focus on DNNs as the current leading data-driven technique, we briefly

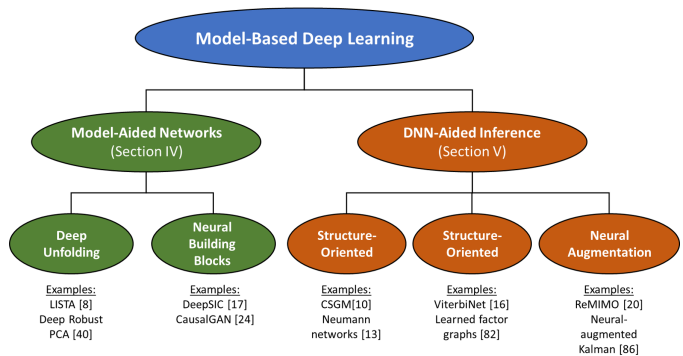


Fig. 2: Division of model-based deep learning techniques into categories and sub-categories.

review basic concepts in deep learning, ensuring that the tutorial is accessible to readers without background in deep learning. We then elaborate on the fundamental strategies for combining model-based methods with deep learning. For each such strategy, we present a few concrete implementation approaches in a systematic manner, including established approaches such as deep unfolding [7], originally proposed in 2010 [8], as well as recently proposed model-based deep learning paradigms such as DNN-aided inference [18] and neural augmentation [21]. For each approach we formulate system design guidelines for a given problem; provide a detailed example from the recent literature; and discuss its properties and use-cases. Each of our detailed examples focuses on a different application in signal processing, communications, and control, demonstrating the breadth and the wide variety of applications that can benefit from such hybrid designs. We conclude the article with a summary and a qualitative comparison of model-based deep learning approaches, along with a description of some future research topics and challenges. We aim to encourage future researchers and practitioners with a signal processing background to study and design model-based deep learning.

The rest of this article is organized as follows: Section II discusses the concepts of model-based methods as compared to data-driven schemes, and how they give rise to the model-based deep learning paradigm. Section III reviews some basics of deep learning, which are used in our presentation of model-based deep learning strategies in the sequel. The main strategies for designing model-based deep learning systems, i.e. model-aided networks and DNN-aided inference, are detailed in a tutorial manner in Sections IV–V, respectively. Finally, we provide a summary and discuss some future research challenges in Section VI.

II. MODEL-BASED VERSUS DATA-DRIVEN INFERENCE

We begin by reviewing the main conceptual differences between model-based and data-driven inference. To that aim, we first present a mathematical formulation of a generic inference problem. Then we discuss how this problem is tackled from a purely model-based perspective as well as from a purely data-driven one, where for the latter we focus on the usage of deep learning as a family of generic data-driven approaches. We then formulate the notion of model-based deep learning based upon these distinct strategies.

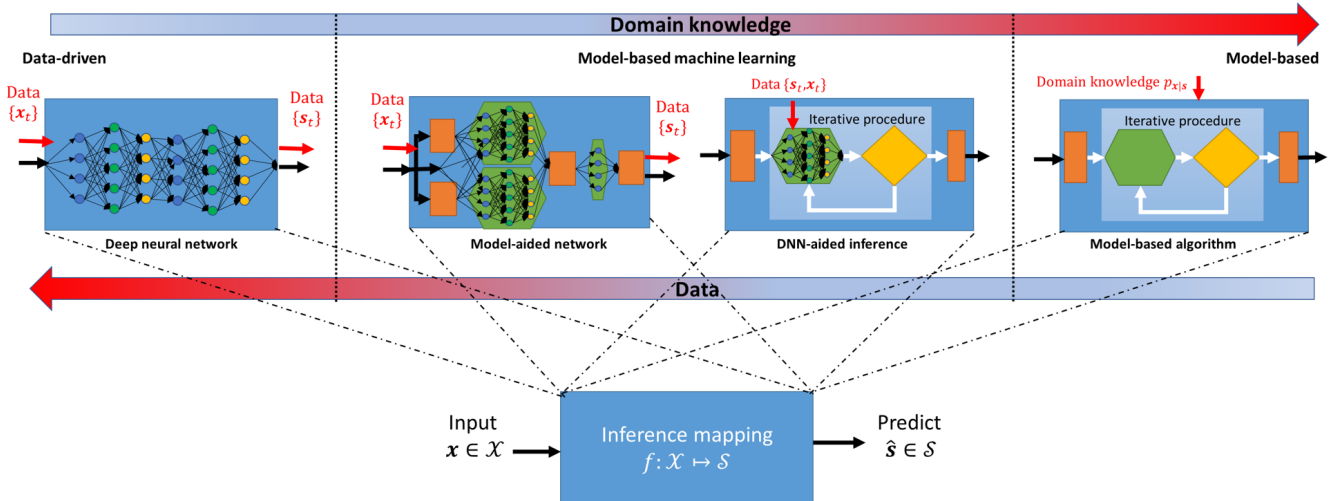


Fig. 3: Illustration of model-based versus data-driven inference. The red arrows correspond to computation performed before the particular inference data is received. For example, compressed sensing using generative models [10] is DNN-aided inference. The data is used to pre-train the generator and the inference procedure corresponds to solving an optimization problem which is not using a network. In contrast a fully supervised inversion method that is training a network to map measurements to reconstructions [22] corresponds to a fully data-driven approach in the far left. Examples of Model-aided networks for inference include Deep unfolding [23], also referred to as *deep unrolling* [9], where a network is trained to perform a fixed number of gradient descent iterations, as well as CausalGANs [24], which embed a known causal graph in a DNN architecture.

A. Inference Systems

The term *inference* refers to the ability to conclude based on evidence and reasoning. While this generic definition can refer to a broad range of tasks, we focus in our description on systems which estimate or make predictions based on a set of observed variables. In this wide family of problems, the system is required to map an input variable $x \in \mathcal{X}$ into a prediction of a label variable $s \in \mathcal{S}$, denoted \hat{s} , where \mathcal{X} and \mathcal{S} are referred to as the *input space* and the *label space*, respectively. An inference rule can thus be expressed as

$$f : \mathcal{X} \mapsto \mathcal{S}, \quad (1)$$

where the fidelity of such a mapping is measured using a loss function, denoted $\mathcal{L}(f)$. Thus, the goal of both model-based methods and data-driven schemes is to design the inference rule $f(\cdot)$ to minimize the loss $\mathcal{L}(f)$ for a given problem. The main difference between these strategies is what information is utilized to tune $f(\cdot)$.

B. Model-Based Methods

Model-based algorithms, also referred to as *hand-designed methods* [25], set their inference rule, i.e. tune f in (1) to minimize the loss function $\mathcal{L}(\cdot)$, based on domain knowledge. The term *domain knowledge* typically refers to prior knowledge of the underlying statistics relating the input x and the label s , such as the generative conditional distribution $p_{x|s}$. Alternatively, domain knowledge can also accommodate deterministic modelling, as commonly used in CS applications [26], [27], where, e.g., x represents linear projections of a sparse s .

Regardless of the nature of the domain knowledge at hand, the main characteristic of model-based methods is that their mapping is dictated by this knowledge. In particular, an

analytical mathematical expression describing the underlying model, e.g., the distribution of x conditioned on s denoted $p_{x|s}$, is required. Model-based algorithms can often provably implement or approach the loss minimizing inference rule at controllable complexity, typically using iterative methods comprised of multiple stages, where each stage involves generic mathematical manipulations and model-specific computations.

Model-based methods do not rely on data to learn their mapping, as illustrated in the right part of Fig. 3, though data is often used to estimate unknown model parameters. In practice, accurate knowledge of the statistical model relating the observations and the desired information is typically unavailable, and thus applying such techniques commonly requires imposing some assumptions on the underlying statistics, which in some cases reflects the actual behavior, but may also constitute a crude approximation of the true dynamics. In the presence of inaccurate model knowledge, either as a result of estimation errors or due to enforcing a model which does not fully capture the environment, the performance of model-based techniques tends to degrade. This limits the applicability of model-based schemes in scenarios where, e.g., $p_{x|s}$ is unknown, costly to estimate accurately, or too complex to express analytically.

C. Data-Driven Schemes

Data-driven systems learn their mapping from data. In a supervised setting, data is comprised of a training set consisting of n_t pairs of inputs and their corresponding labels, denoted $\{x_t, s_t\}_{t=1}^{n_t}$. A leading strategy in data-driven systems, upon which deep learning is based, is to assume some highly-expressive generic parametric model on the mapping in (1). In such cases, the inference rule is dictated by a set of parameters denoted θ , and thus the system mapping is written as f_θ . The conventional application of deep learning implements f_θ using

a DNN architecture, where θ represent the weights of the network. Such highly-parametrized networks can effectively approximate any Borel measurable mapping, as follows from the universal approximation theorem [28, Ch. 6.4.1]. Therefore, by properly tuning their parameters using the training set, as we elaborate in Section III, one should be able to obtain the desirable inference rule.

Unlike model-based algorithms, which are specifically tailored to a given scenario, purely-data-driven methods are model-agnostic, as illustrated in the left part of Fig. 3. The unique characteristics of the specific scenario are encapsulated in the learned weights. The parametrized inference rule, e.g., the DNN mapping, is generic and can be applied to a broad range of different problems. While standard DNN structures are highly model-agnostic and are commonly treated as black boxes, one can still incorporate some level of domain knowledge in the selection of the specific network architecture. For instance, when the input is known to exhibit temporal correlation, architectures based on recurrent neural networks (RNNs) [29] or Transformer [30] are often preferred. Alternatively, in the presence of spatial patterns, one may utilize convolutional layers [31]. An additional method to incorporate domain knowledge into a black box DNN is by pre-processing of the input via, e.g., feature extraction.

The generic nature of data-driven strategies induces some drawbacks, as discussed in detail in Section III in the context of deep learning. Broadly speaking, learning a large number of parameters requires a massive data set to train on. Even when a sufficiently large data set is available, the resulting training procedure is typically lengthy and involves high computational burden. Finally, the black-box nature of the resulting mapping implies that data-driven systems in general lack interpretability, making it difficult to provide performance guarantees and insights into the system operation.

D. Model-Based Deep Learning

Completely separating existing literature into model-based versus data-driven is a daunting, subjective and debatable task. Instead, we focus on some example schemes which clearly lie in the middle ground to give a useful overview of the landscape. The considered families of methods incorporate domain knowledge in the form of an established model-based algorithm which is suitable for the problem at hand, while combining capabilities to learn from data via deep learning techniques.

Model-based deep learning schemes thus tune their mapping of the input \mathbf{x} based on both data, e.g., a labeled training set $\{\mathbf{s}_t, \mathbf{x}_t\}_{t=1}^{n_t}$, as well as some domain knowledge, such as partial knowledge of the underlying distribution $p_{\mathbf{x}|\mathcal{S}}$. Such hybrid data-driven model-aware systems can typically learn their mappings from smaller training sets compared to purely model-agnostic DNNs, and commonly operate without full accurate knowledge of the underlying model, e.g., $p_{\mathbf{x}|\mathcal{S}}$, upon which model-based methods are based.

Techniques for studying and designing of inference rules in a hybrid model-based/data-driven fashion can be divided into two main strategies, as illustrated in Fig. 3. These strategies

may each be further specialized to various different tasks, as we show in the sequel. The first of the two, which we refer to as *model-aided networks*, utilizes model-based methods as a form of domain knowledge in designing a DNN architecture, while using the resultant network for inference. The second strategy, which we call *DNN-aided inference systems*, uses conventional model-based methods for inference, while incorporating learning to make the resultant system more robust and model-agnostic. Since both strategies rely on deep learning tools, we first provide a brief overview of key concepts in conventional deep learning in the following section, after which we elaborate on model-aided networks and DNN-aided inference in Sections IV and V, respectively.

III. BASICS OF DEEP LEARNING

Here, we cover the basics of deep learning required to understand the DNN-based components in the model-based/data-driven approaches discussed later. Our aim is to equip the reader with necessary foundations upon which our formulations of model-aided networks and DNN-aided inference systems are presented.

As described in Subsection II-C, deep learning is a data-driven approach to inference that works by directly *learning* the target inference rule from the input space \mathcal{X} to the label space \mathcal{S} . The target mapping is approximated by a parametrized function $f_\theta : \mathcal{X} \rightarrow \mathcal{S}$ belonging to a fixed family of functions \mathcal{F}_θ specified by a predefined DNN architecture, which is represented by a specific choice of the parameter vector θ .

For a mapping $f_\theta \in \mathcal{F}_\theta$, the quality of its approximation of the unknown target inference rule is given by the *loss function* $\mathcal{L}(\cdot)$, which measures how well f_θ agrees with what can be observed in the available data. The data-driven nature of deep learning thus comes from the dependence of the loss function on the *training data*, i.e., \mathcal{L} is determined by the set $\{\mathbf{s}_t, \mathbf{x}_t\}_{t=1}^{n_t}$. Once the loss function \mathcal{L} and the function class \mathcal{F}_θ are defined, one may attempt to find the optimal function with respect to the loss within \mathcal{F}_θ , i.e.

$$\theta^* = \arg \max_{f_\theta \in \mathcal{F}_\theta} \mathcal{L}(f_\theta). \quad (2)$$

As the optimization in (2) is carried out over the parameter vector θ , we write the loss as $\mathcal{L}(\theta)$ for brevity.

The above formulation naturally gives rise to three fundamental components of deep learning: the DNN *architecture* that defines the function class \mathcal{F}_θ ; the task-specific *loss function* $\mathcal{L}(\theta)$; and the *optimizer* that dictates how to search for the optimal f_θ within \mathcal{F}_θ . Therefore, our review of the basics of deep learning commences with a description of the fundamental architecture and optimizer components in Subsection III-A. We then present several representative tasks along with their corresponding typical loss functions in Subsection III-B. The formulation of these common tasks is exploited in our presentation of the incorporation of deep learning into hybrid model-based/data-driven schemes in Sections IV-V.

A. Deep Learning Preliminaries

The formulation of the data-driven parametric objective in (2) is not unique to deep learning, and is in fact common to

numerous machine learning schemes. The strength of deep learning, i.e., its ability to learn accurate complex mappings from large data sets, is due to its use of DNNs to enable a highly-expressive family of function classes \mathcal{F}_θ , along with dedicated optimization algorithms capable of tuning its parameters from data. In the following we discuss the high level notion of DNNs, followed by a description of how they are optimized.

a) *Neural Network Architecture*: DNNs implement parametric functions comprised of a sequence of differentiable transformations called *layers*, whose composition maps the input to a desired output. Specifically, a DNN f_θ consisting of k layers $\{h_1, \dots, h_k\}$ maps the input \mathbf{x} to the output $\hat{\mathbf{s}} = f_\theta(\mathbf{x}) = h_k \circ \dots \circ h_1(\mathbf{x})$, where \circ denotes function composition. Since each layer h_i is itself a parametric function, the parameters of the entire network f_θ is the union of all of its layers' parameters, and thus f_θ denotes a DNN with parameters θ . The *architecture* of a DNN refers to the specification of its layers $\{h_i\}_{i=1}^k$.

As layers are one of the fundamental building blocks of DNNs, much of deep learning research has been devoted to coming up with layers that perform well in various scenarios. A generic formulation which captures various parametrized layers is that of an affine transformation, i.e., $h(\mathbf{x}) = \mathbf{W}\mathbf{x} + \mathbf{b}$ whose parameters are $\{\mathbf{W}, \mathbf{b}\}$. For instance, in *fully-connected (FC)* layers, also referred to as *dense* layers, one can optimize $\{\mathbf{W}, \mathbf{b}\}$ to take any value. Another extremely common affine transform layer is the *convolutional* layer, where \mathbf{W} is constrained to represent discrete convolution. Such layers are known to yield a highly parameter-efficient mapping that captures important invariances such as translational invariance in image data.

While many commonly used layers including FC and convolutional layers are affine, DNNs rely on the inclusion of *non-linear* layers. If all the layers of a DNN were affine, the composition of all such layers would also be affine, and thus the resulting network would only represent affine functions. For this reason, layers in a DNN are interleaved with *activation functions*, which are simple non-linear functions applied to each dimension of the input separately. Activations are often fixed, i.e., their mapping is not parametric and is thus not optimized in the learning process. Some notable examples of widely-used activation functions include the rectified linear unit (ReLU) defined as $\text{ReLU}(x) = \max\{x, 0\}$ and the sigmoid $\sigma(x) = (1 + \exp(x))^{-1}$.

DNNs allow the function space \mathcal{F}_θ to capture a broad range of functions. In fact, by making the network sufficiently large, one can approximate any Borel measurable mapping, i.e., \mathcal{F}_θ is the space of all Borel measurable functions from \mathcal{X} to \mathcal{S} , as follows from the universal approximation theorem [28, Ch. 6.4.1]. The expressiveness of DNNs combined with the fact that the parameters θ can be learned from data allows trained DNNs to operate reliably in a model-agnostic manner. In fact, highly-parametrized DNNs have demonstrated the ability to disentangle semantic information in complex environments [5]. Optimizing the large amount of parameters of a DNN based on massive volumes of data is feasible, though computationally expensive, due to its sequential structure, as

detailed next.

b) *Choice of Optimizer*: Given a complex neural network f_θ and a loss function $\mathcal{L}(\theta)$, finding a globally optimal θ that minimizes \mathcal{L} is a hopelessly intractable task, especially at the scale of millions of parameters or more. Fortunately, recent success of deep learning has demonstrated that gradient-based optimization methods work surprisingly well despite their inability to find global optima. The simplest such method is *gradient descent*, which iteratively updates the parameters:

$$\theta_{i+1} = \theta_i - \alpha_i \nabla_{\theta} \mathcal{L}(\theta_i), \quad (3)$$

where α_i is the *step size* that may change as a function of the step count i . Since the gradient $\nabla_{\theta} \mathcal{L}(\theta_i)$ is often too costly to compute over the entire training data, it is estimated from a small number of randomly chosen samples (i.e. a mini-batch). The resulting optimization method is called *mini-batch stochastic gradient descent* and belongs to the family of stochastic first-order optimizers.

Stochastic first-order optimization techniques are well-suited for training DNNs because their memory usage grows only linearly with the number of parameters, and they avoid the need to process the entire training data at each step of optimization. Over the years, numerous variations of stochastic gradient descent have been proposed. Many modern optimizers such as RMSProp [32] and Adam [33] use statistics from previous parameter updates to adaptively adjust the step size for each parameter separately (i.e. for each dimension of θ). In general, the interplay between a DNN, an optimizer, and the downstream performance is not yet well-understood and is an active area of research.

B. Common Deep Learning Tasks

As detailed above, the data-driven nature of deep learning is encapsulated in the loss function's dependence on training data. Thus, the loss function not only implicitly defines the task of the resulting system, but also dictates what kind of data is required. Based on the requirements placed on the training data, problems in deep learning largely fall under three different categories: supervised, semi-supervised, and unsupervised. Here we define each category and list some example tasks as well as their typical loss functions.

a) *Supervised Learning*: In supervised learning, the training set consists of a set of input-label pairs $\{(\mathbf{x}_t, \mathbf{s}_t)\}_{t=1}^{n_t} \subset \mathcal{X} \times \mathcal{S}$. Each pair $(\mathbf{x}_t, \mathbf{s}_t)$ satisfies $\mathbf{s}_t = f^*(\mathbf{x}_t)$ for some unknown ground truth mapping f^* . The goal is to have f_θ approximate f^* as accurately as possible by utilizing the given training data. This setting encompasses a wide range of problems including regression, classification, and structured prediction, through a judicious choice of the loss function. Below we review commonly used loss functions for classification and regression tasks.

1) *Classification*: Perhaps one of the most widely-known success stories of DNN, classification (image classification in particular) has remained a core benchmark since the introduction of AlexNet [34]. In this setting, we are given a training set $\{(\mathbf{x}_t, \mathbf{s}_t)\}_{t=1}^{n_t}$ containing input-label pairs, where each \mathbf{x}_t is a fixed-size input, e.g. an image, and \mathbf{s}_t is the one-hot encoding of the class. Such one-hot

encoding of class c can be viewed as a probability vector for a K -way categorical distribution, with $K = |\mathcal{S}|$, with all probability mass placed on class c .

The DNN mapping f_θ for this task is appropriately designed to map an input \mathbf{x}_t to the probability vector $\hat{\mathbf{s}}_t \triangleq f(\mathbf{x}_t) = \langle \hat{s}_{t,1}, \dots, \hat{s}_{t,K} \rangle$, where $\hat{s}_{t,c}$ denotes the c -th component of $\hat{\mathbf{s}}_t$. This parametrization allows for the model to return a soft decision in the form of a categorical distribution over the classes.

A natural choice of loss function for this setting is the *cross-entropy* loss, defined as

$$\mathcal{L}_{\text{CE}}(\theta) = \frac{1}{n_t} \sum_{t=1}^{n_t} \sum_{c=1}^K s_{t,c} (-\log \hat{s}_{t,c}). \quad (4)$$

The loss for a single example is minimized when the two probability vectors \mathbf{s}_t and $\hat{\mathbf{s}}_t$ are equal. Furthermore, for a sufficiently large set of i.i.d. training pairs, the empirical cross entropy loss approaches the expected cross entropy measure, which is minimized when the DNN output matches the true conditional distribution $p_{s|\mathbf{x}}$. Consequently, minimizing the cross-entropy loss encourages the DNN output to match the ground truth label, and its mapping closely approaches the true underlying posterior distribution when properly trained.

One technical but crucial trick in classification setting is the *softmax* function. The formulation of the cross entropy loss (4) implicitly assumes that the DNN returns a valid probability vector, i.e. $\hat{s}_{t,c} \geq 0$ and $\sum_{c=1}^K \hat{s}_{t,c} = 1$. However, there is no guarantee that this will be the case, especially at the beginning of training when the parameters of the DNN are more or less randomly initialized. To guarantee that the DNN mapping yields a valid probability distribution, classifiers typically employ the softmax function (e.g. on top of the output layer), given by:

$$\text{Softmax}(\mathbf{x}) = \left\langle \frac{\exp(\mathbf{x}_1)}{\sum_{i=1}^d \exp(\mathbf{x}_i)}, \dots, \frac{\exp(\mathbf{x}_d)}{\sum_{i=1}^d \exp(\mathbf{x}_i)} \right\rangle.$$

Due to the exponentiation followed by normalization, the output of the softmax function is guaranteed to be a valid probability vector. In effect, the softmax trick removes the burden of outputting a valid probability distribution from the network and improves the stability and speed of the training process.

- 2) *Regression*: Another task where DNNs have been successfully applied is regression, where one attempts to predict a set of continuous variables instead of a categorical one. Here, the labels $\{s_t\}$ in the training data represent some continuous value, e.g. in \mathcal{R} or some specified range $[a, b]$. One simple DNN architecture for regression is a stack of FC layers with activation functions in between as described in Section III-A:

$$\hat{\mathbf{s}}_t \triangleq f_\theta(\mathbf{x}_t) = \sigma \circ h_k \circ \phi \circ \dots \circ \phi \circ h_1(\mathbf{x}_t), \quad (5)$$

where each h_i is an affine layer and ϕ is some activation function. Notably, the last layer h_k must output a single scalar rather than a vector.

Similar to the usage of softmax layer for classification, an appropriate final activation function σ is needed, depending on the range of the variable of interest. For example, when regressing on a strictly positive value, a common choice is $\sigma(x) = \exp(x)$ or the softplus activation $\sigma(x) = \log(1 + \exp(x))$, so that the range of the network f_θ is constrained to be positive reals. When the output is to be limited to an interval $[a, b]$, then one may use the mapping $\sigma(x) = a + (b - a)(1 + \tanh(x))/2$. The most common loss function is the empirical mean-squared error (MSE), as is also widely used statistical modeling in general:

$$\mathcal{L}_{\text{MSE}}(\theta) = \frac{1}{n_t} \sum_{t=1}^{n_t} (s_t - \hat{s}_t)^2. \quad (6)$$

b) *Unsupervised Learning*: In unsupervised learning, we are only given a set of examples $\{\mathbf{x}_t\}_{t=1}^{n_t} \subset \mathcal{X}$ without labels. Since there is no label to predict, unsupervised learning algorithms are often used to discover interesting patterns present in the given data. Common tasks in this setting include clustering, anomaly detection, generative modeling, and compression.

- 1) *Generative models*: One goal in unsupervised learning of a generative model is to train a *generator* network $G_\theta : \mathbf{z} \mapsto \mathbf{x}$ such that the *latent variables* \mathbf{z} , which follow a simple distribution such as standard Gaussian, are mapped to the samples \mathbf{x} in the training data, e.g. images of human faces. A popular type of DNN-based generative model that tries to achieve this goal is *generative adversarial network (GAN)* [35], which has recently shown remarkable success in many domains. Since the training data does not provide the ground truth latent variable \mathbf{z}_t associated with each example \mathbf{x}_t , GANs learn the generative model by employing a *discriminator* network $D_\varphi : \mathcal{X} \rightarrow [0, 1]$, which is a binary classifier trained to distinguish real examples \mathbf{x}_t from the fake examples generated by G . The parameters $\{\theta, \varphi\}$ of the two networks are updated via *adversarial* training, where θ and φ are updated in an alternating manner. Thus the two networks G and D “compete” against each other to achieve opposite goals: G tries to fool the discriminator, whereas D tries to reliably distinguish real examples from the fake ones made by the generator. A typical GAN loss function is the minmax loss, given by

$$\mathcal{L}_{\text{MinMax}}(\theta, \varphi) = \frac{1}{n_t} \sum_{t=1}^{n_t} \log D_\varphi(\mathbf{x}_t) + \log(1 - D_\varphi(G_\theta(\mathbf{z}_t))), \quad (7)$$

where the latent variables $\{\mathbf{z}_t\}$ are drawn from its known prior distribution for each mini-batch.

Among currently available deep generative models, GANs achieve the best sample quality at an unprecedented resolution. For example, the current state-of-the-art model StyleGAN2 [36] is able to generate high-resolution (1024×1024) images that are nearly indistinguishable from real photos to a human observer. That said, GANs do come with several disadvantages as

well. The adversarial training procedure is known to be unstable, and many tricks are necessary in practice to train a large GAN. Also because GANs do not offer any probabilistic interpretation, it is difficult to objectively evaluate the quality of a GAN.

- 2) *Autoencoders*: Another well-studied task in unsupervised learning is the training of an *autoencoder*, which has many uses such as dimensionality reduction and representation learning. An autoencoder consists of two neural networks: an *encoder* $f_{\text{enc}} : \mathcal{X} \mapsto \mathcal{Z}$ and a *decoder* $f_{\text{dec}} : \mathcal{Z} \mapsto \mathcal{X}$, where \mathcal{Z} is some predefined latent space. The primary goal of an autoencoder is to reconstruct a signal \mathbf{x} from itself by mapping it through $f_{\text{dec}} \circ f_{\text{enc}}$. The output of the encoder $f_{\text{enc}}(\mathbf{x})$ is often called the *code* or the *latent variable*, and the output of the decoder $f_{\text{dec}}(f_{\text{enc}}(\mathbf{x}))$ is called the *reconstruction* of \mathbf{x} . The task of autoencoding may seem pointless at first; indeed one can trivially recover \mathbf{x} by setting $\mathcal{Z} = \mathcal{X}$ and $f_{\text{enc}}, f_{\text{dec}}$ to be identity functions. The interesting case is when the latent space \mathcal{Z} is restricted to be lower-dimensional than \mathcal{X} , e.g. $\mathcal{X} = \mathbb{R}^n$ and $\mathcal{Z} = \mathbb{R}^m$ for some $m < n$. This constraint forces the encoder to map its input into a more compact representation, while retraining enough information so that the reconstruction is as close to the original input as possible. The most common distortion metric used to measure the quality of reconstruction is the MSE loss. Under this setting, we obtain the following loss function for training:

$$\mathcal{L}_{\text{MSE}}(f_{\text{enc}}, f_{\text{dec}}) = \frac{1}{n_t} \sum_{t=1}^{n_t} \|\mathbf{x}_t - f_{\text{dec}}(f_{\text{enc}}(\mathbf{x}_t))\|_2^2 \quad (8)$$

Due to the constraint on \mathcal{Z} , the latent variable $\mathbf{z} = f_{\text{enc}}(\mathbf{x})$ can be seen as a continuous low-dimensional representation of \mathbf{x} , even when \mathcal{X} is discrete or high-dimensional. When \mathbf{z} is appropriately quantized, it can also be used to implement a learned lossy compressor of samples from \mathcal{X} .

Many variations of the above autoencoder formulation have been proposed and extensively studied in the deep learning literature. For example, a *denoising* autoencoder [37] receives a noisy input example and tries to reconstruct the noiseless version of it, leading to a latent representation that is robust to input noise. Another popular architecture is the variational autoencoder (VAE) [38], in which the latent variable \mathbf{z} is stochastic, and thus the decoder can be used as a learned generative model.

- c) *Semi-supervised Learning*: Semi-supervised learning lies in the middle ground between the above two categories, where one typically has access to a large amount of unlabeled data and a small set of labeled data. The goal is to leverage the unlabeled data to improve performance on some supervised task to be trained on the labeled data. As labeling data is often a very costly process, semi-supervised learning provides a way to quickly learn desired inference rules without having to label all of the available unlabeled data points.

IV. MODEL-AIDED NETWORKS

Model-aided networks implement model-based deep learning by using model-aware algorithms to design deep architectures. Here, structures exhibited by model-based methods for the problem at hand are utilized in designing a DNN architecture, while using the resultant network for inference. Unlike conventional model-agnostic deep learning discussed in Section III, model-aided networks utilize a unique DNN structure designed for the specific task by imitating the process carried out by a model-based algorithm, which has full knowledge of the underlying model, either statistical or deterministic.

Broadly speaking, model-aided networks implement the inference system using a DNN, similar to conventional deep learning. Nonetheless, instead of applying generic off-the-shelf DNNs, the rationale here is to tailor the architecture specifically for the scenario of interest. In particular, the rationale in model-aided networks is to obtain this dedicated architecture by identifying structures in a model-based algorithm one would have utilized for the problem given full domain knowledge and sufficient computational resources. Such structures can be given in the form of an iterative representation of the model-based algorithm, as exploited by *deep unfolding* detailed in Subsection IV-A, or via a block diagram algorithmic representation, which *neural building blocks* rely upon, as presented in Subsection IV-B. The dedicated neural network is then obtained by tuning a parametric architecture whose specific layers, activations, intermediate mathematical manipulations, and interconnections imitate the operations of the model-based algorithm, as illustrated in Fig. 4. We next elaborate on the main approaches for designing model-aided networks, namely, deep unfolding and neural building blocks, in Subsection IV-A and IV-B, respectively.

A. Deep Unfolding

Deep unfolding [23], also referred to as *deep unrolling* [9], is a method for converting an iterative algorithm into a DNN by designing each layer of the network to resemble a single iteration. Deep unfolding was originally proposed by Greger and LeCun in [8], where a deep architecture was designed to learn to carry out the iterative soft thresholding algorithm (ISTA) for sparse recovery. Deep unfolded networks have since been applied in various applications in image denoising [7], [39], [40], sparse recovery [9], [25], [41], dictionary learning [42], [43], communications [19], [44]–[47], ultrasound [48], [49], and super resolution [50]–[52]. A recent review can be found in [7].

Design Outline: The application of deep unfolding to design a model-aided deep network is based on the following steps:

- 1) Identify an iterative optimization algorithm which is useful for the problem at hand. For instance, recovering a sparse vector from its projections corrupted by low-rank clutter and noise can be tackled using the generalization of ISTA for robust principal component analysis (PCA) [53], unfolded in [40], as described in the sequel.
- 2) Fix a number of iterations in the optimization algorithm.
- 3) Design the layers to imitate the free parameters of each iteration in a trainable fashion.

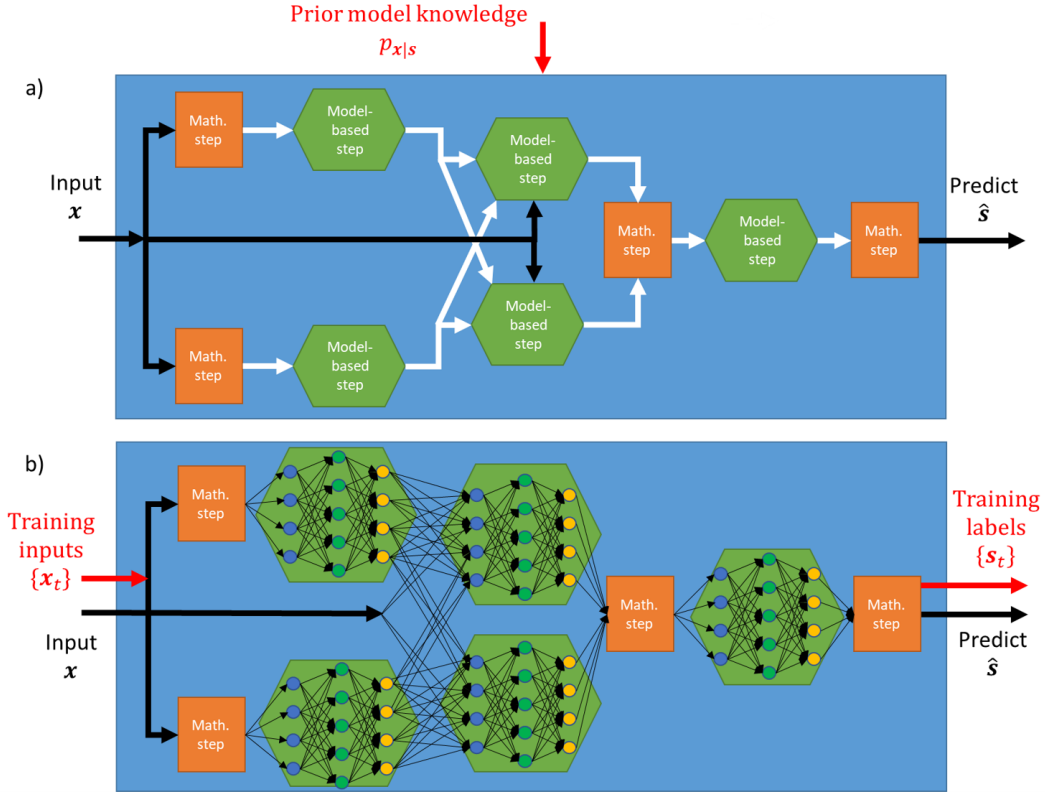


Fig. 4: Model-aided DNN illustration: *a)* a model-based algorithm comprised of a series of model-aware computations and generic mathematical steps; *b)* A DNN whose architecture and internal inter-connections are designed based on the model-based algorithm.

- 4) Train the overall resulting network in an end-to-end fashion.

We next demonstrate how this rationale is translated into a concrete architecture, using the example of deep unfolded robust PCA proposed in [40].

Example: Deep Unfolded Robust PCA: Robust PCA refers to the problem of recovering a sparse matrix where the measurements are corrupted by low-rank clutter as well as noise. Such scenarios are commonly encountered, e.g., in medical imaging. In the following, we first formulate the robust PCA system model and objective, after which we discuss the generalization of the ISTA algorithm for such setups, and show how it is unfolded into the deep unfolded robust PCA architecture proposed in [40].

a) System Model: Consider the recovery of a sparse matrix \mathbf{S} based on an observed data matrix \mathbf{X} , which are both complex-valued matrices. In particular, the measurements are related to the desired sparse matrix via

$$\mathbf{X} = \mathbf{H}_1 \mathbf{L} + \mathbf{H}_2 \mathbf{S} + \mathbf{W}. \quad (9)$$

Here, \mathbf{H}_1 and \mathbf{H}_2 are measurement matrices of appropriate dimensions; \mathbf{L} is a low-rank clutter matrix; and \mathbf{W} is an additive noise signal. Observations obeying the structure in (14) are commonly encountered in medical imaging, e.g. where tissues induce high spatial-temporal coherence, and thus typically obey a low-rank representation, while blood vessels are usually sparsely populated and thus can be represented as a

sparse matrix over multiple temporal snapshots. Consequently, we focus in this example on the recovery of blood vessel echos in ultrasound imaging, which translates to the estimation of \mathbf{S} in (9), being the problem considered in [40].

The domain knowledge that \mathbf{S} is sparse and that \mathbf{L} is low rank implies that their recovery can be obtained by solving the following relaxed optimization problem [53]:

$$\min_{\mathbf{S}, \mathbf{L}} \|\mathbf{X} - \mathbf{H}_1 \mathbf{L} + \mathbf{H}_2 \mathbf{S}\|_F^2 + \lambda_1 \|\mathbf{L}\|_* + \lambda_2 \|\mathbf{S}\|_{1,2}, \quad (10)$$

where $\|\cdot\|_F$, $\|\cdot\|_*$, and $\|\cdot\|_{1,2}$ are the Frobenious, nuclear, and mixed $\ell_{1,2}$ norms, while λ_1 and λ_2 are regularization coefficients promoting low rankness of \mathbf{L} and sparsity of \mathbf{S} , respectively.

b) Generalized ISTA: The robust PCA objective formulation in (10) can be solved by the generalization of ISTA to the matrix domain. This model-based algorithm, which requires full knowledge of the model equation (9), and particularly the measurement matrices $\mathbf{H}_1, \mathbf{H}_2$, operates in an iterative manner with a fixed step-size μ . In each iteration q , it updates its local estimates of \mathbf{L} and \mathbf{S} based on their estimates produced in the previous iteration by taking the proximal mappings corresponding to the nuclear and $\ell_{1,2}$ norms in (10).

In particular, the ISTA update equations are given by

$$\hat{\mathbf{L}}_{q+1} = \text{SVT}_{\lambda_1} \left\{ \left(\mathbf{I} - \frac{1}{\mu} \mathbf{H}_1^H \mathbf{H}_1 \right) \hat{\mathbf{L}}_q - \mathbf{H}_1^H \mathbf{H}_2 \hat{\mathbf{S}}_q + \mathbf{H}_1^H \mathbf{X} \right\}, \quad (11a)$$

$$\hat{\mathbf{S}}_{q+1} = \text{T}_{\lambda_2} \left\{ \left(\mathbf{I} - \frac{1}{\mu} \mathbf{H}_2^H \mathbf{H}_2 \right) \hat{\mathbf{S}}_q - \mathbf{H}_2^H \mathbf{H}_1 \hat{\mathbf{L}}_q + \mathbf{H}_2^H \mathbf{X} \right\}, \quad (11b)$$

where T_{λ} is the soft thresholding operator, given by $\text{T}_{\lambda}(\mathbf{X}) = (1 - \lambda/\|\mathbf{X}\|_2)^+ \mathbf{X}$, with $(a)^+ \triangleq \max(a, 0)$, and SVT_{λ} is the singular value thresholding operator, which for a matrix \mathbf{X} with singular value decomposition $\mathbf{X} = \mathbf{U} \text{diag}(\sigma_1, \dots, \sigma_r) \mathbf{V}^H$ is defined as $\text{SVT}_{\lambda}(\mathbf{X}) = \mathbf{U} \text{diag}((\sigma_1 - \lambda)^+, \dots, (\sigma_r - \lambda)^+) \mathbf{V}^H$.

c) Deep Unfolded Robust PCA: The hybrid data-driven/model-based architecture proposed in [40] imitates the ISTA procedure without requiring prior knowledge of the measurement matrices $\mathbf{H}_1, \mathbf{H}_2$ or the thresholding parameters. To formulate the deep unfolded robust PCA system, we first fix a number of iterations Q . Next, we design a DNN with Q layers, where each layer imitates a single iteration of (11) in a trainable manner.

Architecture: Deep unfolded robust PCA builds upon the observation that each ISTA iteration consists of two affine mappings of the previous estimates and the measurements, that are fed into the non-linear proximal mappings SVT_{λ_1} and T_{λ_2} . Therefore, letting $\hat{\mathbf{L}}_q$ and $\hat{\mathbf{S}}_q$ be the estimates of \mathbf{L} and \mathbf{S} produced at the output the q th layer, the $(q+1)$ th unfolded iteration is represented as two learned affine mappings, which operate on \mathbf{X} , \mathbf{L}_q , and \mathbf{S}_q , followed by activation functions based on the corresponding proximal mappings. Consequently, the operation of the unfolded iteration can be written as

$$\hat{\mathbf{L}}_{q+1} = \text{SVT}_{\lambda_1^{(q)}} \left\{ \mathbf{P}_5^{(q)} \hat{\mathbf{L}}_q + \mathbf{P}_3^{(q)} \hat{\mathbf{S}}_q + \mathbf{P}_1^{(q)} \mathbf{X} \right\}, \quad (12a)$$

$$\hat{\mathbf{S}}_{q+1} = \text{T}_{\lambda_2^{(q)}} \left\{ \mathbf{P}_6^{(q)} \hat{\mathbf{L}}_q + \mathbf{P}_4^{(q)} \hat{\mathbf{S}}_q + \mathbf{P}_2^{(q)} \mathbf{X} \right\}. \quad (12b)$$

Here, the learnable affine mappings are implemented using convolutional layers, i.e., $\{\mathbf{P}_i^{(q)}\}$ represent the trainable convolution kernels, and the overall network parameters are $\theta = \{\{\mathbf{P}_i^{(q)}\}_{i=1}^6, \lambda_1^{(q)}, \lambda_2^{(q)}\}_{q=1}^Q$. The resulting deep network is depicted in Fig. 5, in which $\hat{\mathbf{L}}_0$ and $\hat{\mathbf{S}}_0$ are set to some initial guess, and the output after Q iterations, denoted $\hat{\mathbf{S}}_Q$, is used as the estimate of the desired sparse matrix \mathbf{S} .

Training: To tune θ , the overall network is trained in an end-to-end manner to minimize the empirical Frobenius norm loss. Since the algorithm estimates the low rank clutter matrix \mathbf{L} in addition to the sparse matrix \mathbf{S} , the training accounts for the errors in both estimates. Consequently, the training set here is comprised of pairs of observed matrices along with their corresponding \mathbf{S} and \mathbf{L} matrices. In particular, by letting $\{\mathbf{S}_t, \mathbf{L}_t, \mathbf{X}_t\}_{t=1}^{n_t}$ denote the training set, the loss function optimized by the deep unfolded robust PCA is

$$\mathcal{L}(\theta) = \frac{1}{n_t} \sum_{t=1}^{n_t} \|\mathbf{S}_t - \hat{\mathbf{S}}_Q(\mathbf{X}_t; \theta)\|_F^2 + \|\mathbf{L}_t - \hat{\mathbf{L}}_Q(\mathbf{X}_t; \theta)\|_F^2, \quad (13)$$

where $\hat{\mathbf{S}}_Q(\mathbf{X}_t; \theta)$ and $\hat{\mathbf{L}}_Q(\mathbf{X}_t; \theta)$ are the outputs of the unfolded DNN with parameters θ and input \mathbf{X}_t .

Quantitative Results: An experimental study of deep unfolded robust PCA, demonstrating the ability of deep unfolding to carry out inference both quickly and reliably, is presented in Fig. 6. In particular, Fig. 6(c) shows the recovered ultrasound (contrast agents) image from a cluttered image (Fig. 6(a)) achieved using deep unfolded robust PCA with $Q = 10$ layers trained using $n_t = 4800$ images. Comparing the recovered image to the ground-truth in Fig. 6(b) demonstrates the accuracy in using a DNN to imitate the operations of the generalized ISTA algorithm in a learned fashion. Furthermore, the fact that the unfolded network learns its parameters from data for each layer allows it to infer with a notably reduced number of layers compared to the corresponding number of iterations required by the model-based algorithm, which utilizes its full domain knowledge in applying the hard-coded iterative procedure. This is illustrated in Fig. 6(d) which demonstrates that the trained unfolded network can achieve with only a few layers an MSE accuracy which the model-based fast ISTA of [54], [55] does not approach even in 50 iterations.

Discussion: Deep unfolding incorporates model-based domain knowledge to obtain a dedicated DNN design which resembles an iterative optimization algorithm. Compared to conventional DNNs discussed in Section III, unfolded networks are typically interpretable, and tend to have a smaller number of parameters, and can thus be trained more quickly [7], [44]. Nonetheless, these deep networks are still quite highly parametrized and require a large volume of training data.

One of the key properties of unfolded networks is their reliance on model knowledge. For example, one must know that the relationship between the observed image \mathbf{X} and the desired image \mathbf{S} takes the form (9), as well as that \mathbf{S} and \mathbf{L} are sparse and low-rank, respectively, in order to formulate the ISTA iterations (11), which in turn are unfolded into the trainable layers in (12). The model-awareness of deep unfolding has its advantages and drawbacks. When the model is accurately known, deep unfolding essentially incorporates it into the DNN architecture, as opposed to conventional black-box DNNs which must learn it from data. However, this approach does not exploit the model-agnostic nature of deep learning, and thus may lead to degraded performance when the true relationship between the measurements and the desired quantities deviates from the model assumed in design, e.g., (9). Nonetheless, training an unfolded network designed with a mismatched model using data corresponding to the true underlying scenario typically yields more accurate inference compared to the model-based iterative algorithm with the same model-mismatch, as the unfolded network can learn to compensate for this mismatch from data.

Another advantage of deep unfolding over model-based optimization is in inference speed. For instance, as illustrated in the quantitative example above, unfolding the model-based ISTA iterations into a DNN allows to infer with much fewer layers compared to the number of iterations required for the fast ISTA implementation to converge. This advantage is not unique to the specific example of deep unfolded robust

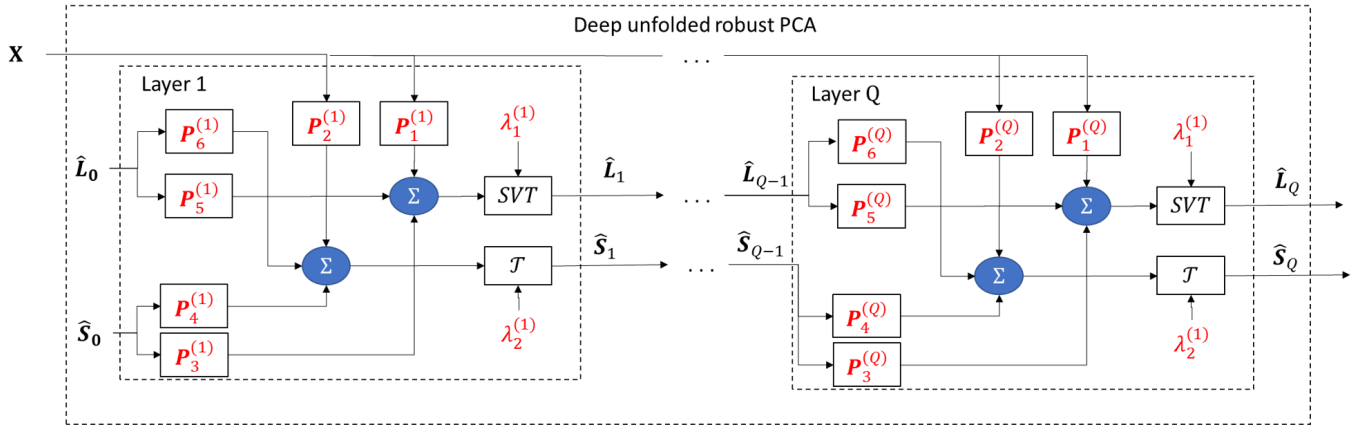


Fig. 5: Deep unfolded robust PCA illustration. Parameters in red fonts are learned in training.

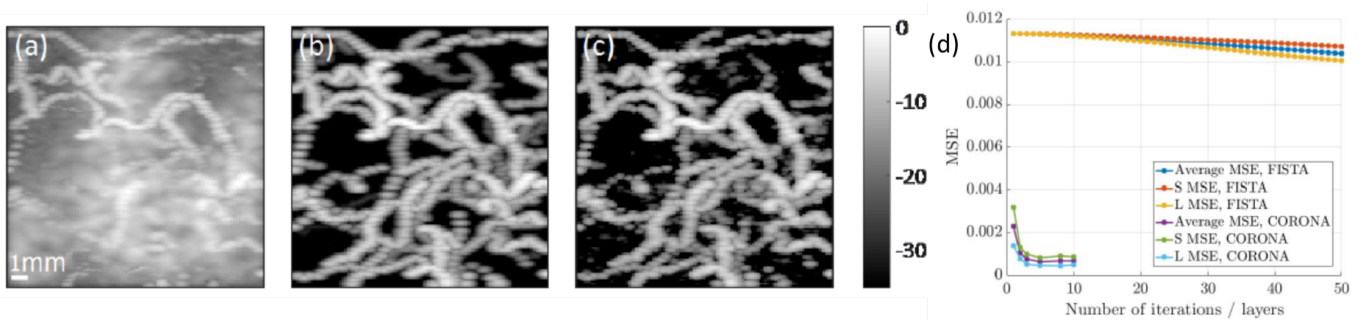


Fig. 6: Experimental results for recovering ultrasound contrast agents (sparse matrix S) from cluttered maximum intensity projection images (observed matrix X): *a*) the observed image X ; *b*) the ground-truth sparse S ; *c*) image recovered by deep unfolded robust PCA; *d*) MSE versus iterations/layers of deep unfolded robust PCA (CORONA) compared to the fast ISTA method [54]. Figures reproduced from [40] with authors' permission.

PCA compared to the generalized ISTA optimization discussed here; similar observations have been made in various unfolded algorithms [19], [50], [56].

Finally, we note that some applications of deep unfolding, such as the unfolded symbol detectors of [19], [46], require knowledge not only of the system model, i.e., that the relationship between the input and the labels are given by, e.g., (9), but also of its parameters, which are H_1 , H_2 , and the distribution of W for the robust PCA example. Such unfolded architectures utilize these parameters as part of their learned layers. While this approach allows to exploit the presence of full domain knowledge, it implies that when these parameters are not known, additional mechanisms must be incorporated in order to estimate them separately, as proposed in [45]. Although using the true (or estimated) model parameters in the unfolded network results in an architecture which closely follows the iterative algorithm, learning the system model parameters commonly enables achieving improved performance compared to using their true value, assuming sufficient training is provided. This is because the learning process can bypass losses inherently induced by the optimization algorithm, e.g., due to some small level of model mismatch.

B. Neural Building Blocks

An alternative approach to design model-aided networks, which can be treated as a generalization of deep unfolding,

is based on representing a model-based algorithm suitable for the problem at hand, or alternatively prior knowledge of an underlying statistical model, as an interconnection of distinct building blocks. Neural building blocks implement a DNN comprised of multiple sub-networks. Each module is designed to carry out the specific computations of the different building blocks constituting the model-based algorithm, as done in [17], [57], or to capture a known statistical relationship, as utilized in CausalGANs [24].

Neural building blocks are designed for scenarios which are tackled using iterative algorithms, or known to be statistically captured using a flow diagram, that can be represented as a sequential interconnection of building blocks. In particular, deep unfolding can be obtained as a special case of neural building blocks, where the building blocks are interconnected in a sequential fashion and implemented using a single layer. However, the generalization of neural building blocks compared to deep unfolding is not encapsulated merely in its ability to implement non-sequential interconnections algorithmic building blocks in a learned fashion, but also in the identification of the specific task of each block, as well as the ability to convert known statistical relationships such as causal graphs into dedicated DNN architecture.

When each algorithmic block has a well-defined task in the model-based algorithm, its data-driven implementation,

obtained by replacing each block with a dedicated DNN, can be trained in either of the following manners: The first is the straight-forward approach of training in an end-to-end fashion, as in conventional deep learning; Alternatively, since the purpose of each building block is dictated by the model-based method, one can train each DNN block separately. The main advantage of the former is its ability to learn a more accurate inference rule given sufficient training, as all the parameters are trained jointly. The advantage of the latter strategy stems from its ability to learn from smaller data sets, as the same data is reused for training each block individually, whose number of trainable parameters is only a portion of that of the overall network, which has to be learned jointly when training end-to-end. In addition, training each block separately facilitates adding and removing blocks, when such operations are required in order to adapt the inference rule.

Design Outline: The application of neural building blocks to design a model-aided deep network is based on the following steps:

- 1) Identify an algorithm or a flow-chart structure which is useful for the problem at hand, and can be decomposed into multiple building blocks.
- 2) Identify which of these building blocks should be learned from data, and what is their concrete task.
- 3) Design a dedicated neural network for each building block capable of learning to carry out its specific task.
- 4) Train the overall resulting network, either in an end-to-end fashion or by training each building block network individually.

We next demonstrate how one can design a model-aided network comprised of neural building blocks. Our example focuses on symbol detection in flat multiple-input multiple-output (MIMO) channels, where we consider the data-driven implementation of the iterative soft interference cancellation (SIC) algorithm of [58], which is the DeepSIC algorithm proposed in [17].

Example: DeepSIC for MIMO Detection: DeepSIC is a hybrid model-based/data-driven implementation of the iterative SIC method [58], which is suitable for linear Gaussian channels. However, unlike its model-based counterpart, and alternative deep MIMO receivers [19], [44], [45], DeepSIC is not particularly tailored for linear Gaussian channels, and can be utilized in various flat MIMO channels. We formulate DeepSIC by first discussing the statistical model for which the iterative SIC method, i.e., the model-based algorithm DeepSIC originates from, is derived. We then review the model-based iterative SIC, and present DeepSIC as its data-driven implementation.

a) System Model: Iterative SIC is a method for symbol detection in linear memoryless MIMO Gaussian channels. The task is to recover the K -dimensional vector \mathbf{s} from the $N \times 1$ observations \mathbf{x} , which are related via:

$$\mathbf{x} = \mathbf{H}\mathbf{s} + \mathbf{w}. \quad (14)$$

Here, \mathbf{H} is a known deterministic $N \times K$ channel matrix, and \mathbf{w} consists of N i.i.d Gaussian random variables (RVs). For our presentation we consider the case in which the

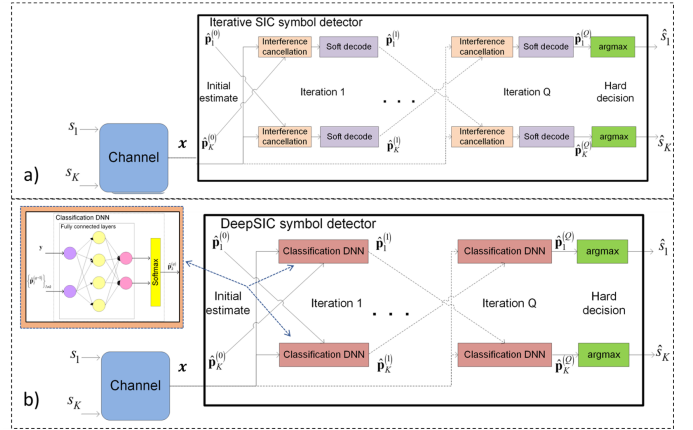


Fig. 7: Iterative SIC illustration: a) model-based method; b) DeepSIC.

entries of \mathbf{s} are symbols generated from a binary phase shift keying (BPSK) constellation in a uniform i.i.d. manner, i.e., $\mathcal{S} = \{\pm 1\}$. In this case the maximum a-posteriori probability (MAP) rule given an observation \mathbf{x} becomes the minimum distance estimate, given by

$$\hat{\mathbf{s}} = \arg \min_{\mathbf{s} \in \{\pm 1\}^K} \|\mathbf{x} - \mathbf{H}\mathbf{s}\|^2. \quad (15)$$

b) Iterative Soft Interference Cancellation: The iterative SIC algorithm proposed in [58] is a MIMO detection method that combines multi-stage interference cancellation with soft decisions. The detector operates in an iterative fashion where, in each iteration, an estimate of the conditional probability mass function (PMF) of s_k , which is the k th entry of \mathbf{s} , given the observed \mathbf{x} , is generated for every symbol $k \in \{1, 2, \dots, K\} := \mathcal{K}$ using the corresponding estimates of the interfering symbols $\{s_l\}_{l \neq k}$ obtained in the previous iteration. Iteratively repeating this procedure refines the conditional distribution estimates, allowing the detector to accurately recover each symbol from the output of the last iteration. This iterative procedure is illustrated in Fig. 7(a).

To formulate the algorithm, we consider the Gaussian MIMO channel in (14). Iterative SIC consists of Q iterations. Each iteration indexed $q \in \{1, 2, \dots, Q\} \triangleq \mathcal{Q}$ generates K distribution vectors $\hat{\mathbf{p}}_k^{(q)}$ of size $M \times 1$, where $k \in \mathcal{K}$. These vectors are computed from the observed \mathbf{x} as well as the distribution vectors obtained at the previous iteration, $\{\hat{\mathbf{p}}_k^{(q-1)}\}_{k=1}^K$. The entries of $\hat{\mathbf{p}}_k^{(q)}$ are estimates of the distribution of s_k for each possible symbol in \mathcal{S} , given the observed \mathbf{x} and assuming that the interfering symbols $\{s_l\}_{l \neq k}$ are distributed via $\{\hat{\mathbf{p}}_l^{(q-1)}\}_{l \neq k}$. Every iteration consists of two steps, carried out in parallel for each user: *Interference cancellation*, and *soft decoding*. Focusing on the k th user and the q th iteration, the interference cancellation stage first computes the expected values and variances of $\{s_l\}_{l \neq k}$ based on the estimated PMF $\{\hat{\mathbf{p}}_l^{(q-1)}\}_{l \neq k}$. The contribution of the interfering symbols from \mathbf{x} is then canceled by replacing them with $\{e_l^{(q-1)}\}$ and subtracting their resulting term. Letting \mathbf{h}_l be the l th column

of \mathbf{H} , the interference canceled channel output is given by

$$\mathbf{z}_k^{(q)} = \mathbf{x} - \sum_{l \neq k} \mathbf{h}_l e_l^{(q-1)}. \quad (16)$$

Substituting the channel output \mathbf{x} into (16), the realization of the interference canceled $\mathbf{z}_k^{(q)}$ is obtained.

To implement soft decoding, it is assumed that $\mathbf{z}_k^{(q)} = \mathbf{h}_k s_k + \tilde{\mathbf{w}}_k^{(q)}$, where the interference plus noise term $\tilde{\mathbf{w}}_k^{(q)}$ obeys a zero-mean Gaussian distribution, independent of s_k , with covariance $\Sigma_k^{(q)} = \sigma_w^2 \mathbf{I}_K + \sum_{l \neq k} v_l^{(q-1)} \mathbf{h}_l \mathbf{h}_l^T$, where σ_w^2 is the noise variance. Combining this assumption with (16), the conditional distribution of $\mathbf{z}_k^{(q)}$ given $s_k = \alpha_j$ is multivariate Gaussian with mean value $\mathbf{h}_k \alpha_j$ and covariance $\Sigma_k^{(q)}$. The conditional PMF of s_k given \mathbf{x} is then approximated from the conditional distribution of $\mathbf{z}_k^{(q)}$ given s_k via Bayes theorem. After the final iteration, the symbols are decoded by taking the symbol that maximizes the estimated conditional distribution for each user.

c) DeepSIC: Iterative SIC is specifically designed for linear channels of the form (14). In particular, the interference cancellation step in (16) requires the contribution of the interfering symbols to be additive. Furthermore, it requires accurate complete knowledge of the underlying statistical model, i.e., of (14). DeepSIC learns to implement the iterative SIC from data as a set of neural building blocks, thus circumventing these limitations of its model-based counterpart.

Architecture: The iterative SIC can be viewed as a set of interconnected basic building blocks, each implementing the two stages of interference cancellation and soft decoding, as illustrated in Fig. 7(a). While the block diagram in Fig. 7(a) is ignorant of the underlying channel model, the basic building blocks are model-dependent. Although each of these basic building blocks consists of two sequential procedures which are completely channel-model-based, we note that the purpose of these computations is to carry out a classification task. In particular, the k th building block of the q th iteration, $k \in \mathcal{K}$, $q \in \mathcal{Q}$, produces $\hat{\mathbf{p}}_k^{(q)}$, which is an estimate of the conditional PMF of s_k given \mathbf{x} based on $\{\hat{\mathbf{p}}_l^{(q-1)}\}_{l \neq k}$. Such computations are naturally implemented by classification DNNs, e.g., FC networks with a softmax output layer. Embedding these conditional PMF computations into the iterative SIC block diagram in Fig. 7(a) yields the overall receiver architecture depicted in Fig. 7(b).

A major advantage of using classification DNNs as the basic building blocks in Fig. 7(b) stems from the fact that such methods are capable of accurately computing conditional distributions in complex non-linear setups without requiring a-priori knowledge of the channel model and its parameters. Consequently, when these building blocks are trained to properly implement their classification task, the receiver essentially realizes iterative SIC for arbitrary channel models in a data-driven fashion.

Training: In order for DeepSIC to reliably implement symbol detection, its building block classification DNNs must be properly trained. Two possible training approaches are considered based on a labeled set of n_t samples $\{\mathbf{s}_t, \mathbf{x}_t\}_{t=1}^{n_t}$:

(i) End-to-end training: The first approach jointly trains

the entire network, i.e., all the building block DNNs. Since the output of the deep network is the set of conditional distributions $\{\hat{\mathbf{p}}_k^{(Q)}\}_{k=1}^K$, where each $\hat{\mathbf{p}}_k^{(Q)}$ is used to estimate S_k , we adopt the sum cross entropy as the training objective. Let $\boldsymbol{\theta}$ be the network parameters, and $\hat{\mathbf{p}}_k^{(Q)}(\mathbf{x}, \alpha; \boldsymbol{\theta})$ be the entry of $\hat{\mathbf{p}}_k^{(Q)}$ corresponding to $S_k = \alpha$ when the input to the network parameterized by $\boldsymbol{\theta}$ is \mathbf{x} . The sum cross entropy loss is

$$\mathcal{L}(\boldsymbol{\theta}) = \frac{1}{n_t} \sum_{t=1}^{n_t} \sum_{k=1}^K -\log \hat{\mathbf{p}}_k^{(Q)}(\mathbf{x}_t, (\mathbf{s}_t)_k; \boldsymbol{\theta}). \quad (17)$$

Training the interconnection of building block DNNs in Fig. 7(b) in an end-to-end manner based on the loss (17) jointly updates the coefficients of all the $K \cdot Q$ building block DNNs. For a large number of symbols, i.e., large K , training so many parameters simultaneously is expected to require a large labeled set.

(ii) Sequential training: The fact that DeepSIC is implemented as an interconnection of neural building blocks, implies that each block can be trained with a reduced number of training samples. Specifically, the goal of each building block DNN does not depend on the iteration index: The k th building block of the q th iteration outputs a soft estimate of S_k for each $q \in \mathcal{Q}$. Therefore, each building block DNN can be trained individually, by minimizing the conventional cross entropy loss. To formulate this objective, let $\boldsymbol{\theta}_k^{(q)}$ represent the parameters of the k th DNN at iteration q , and write $\hat{\mathbf{p}}_k^{(q)}(\mathbf{x}, \{\hat{\mathbf{p}}_l^{(q-1)}\}_{l \neq k}, \alpha; \boldsymbol{\theta}_k^{(q)})$ as the entry of $\hat{\mathbf{p}}_k^{(q)}$ corresponding to $S_k = \alpha$ when the DNN parameters are $\boldsymbol{\theta}_k^{(q)}$ and its inputs are \mathbf{x} and $\{\hat{\mathbf{p}}_l^{(q-1)}\}_{l \neq k}$. The cross entropy loss is

$$\mathcal{L}(\boldsymbol{\theta}_k^{(q)}) = \frac{-1}{n_t} \sum_{t=1}^{n_t} \log \hat{\mathbf{p}}_k^{(q)}(\tilde{\mathbf{x}}_t, \{\hat{\mathbf{p}}_{t,l}^{(q-1)}\}_{l \neq k}, (\tilde{\mathbf{s}}_t)_k; \boldsymbol{\theta}_k^{(q)}), \quad (18)$$

where $\{\hat{\mathbf{p}}_{t,l}^{(q-1)}\}$ represent the estimated probabilities associated with \mathbf{x}_i computed at the previous iteration. The problem with training each DNN individually is that the soft estimates $\{\hat{\mathbf{p}}_{t,l}^{(q-1)}\}$ are not provided as part of the training set. This challenge can be tackled by training the DNNs corresponding to each layer in a sequential manner, where for each layer the outputs of the trained previous iterations are used as the soft estimates fed as training samples.

Quantitative Results: Two experimental studies of DeepSIC taken from [17] are depicted in Fig. 8. These results compare the symbol error rate (SER) achieved by DeepSIC which learns to carry out $Q = 5$ SIC iterations from $n_t = 5000$ labeled samples. In particular, Fig. 8a considers a Gaussian channel of the form (14) with $K = N = 32$, resulting in MAP detection being computationally infeasible, and compares DeepSIC to the model-based iterative SIC as well as the data-driven DetNet architecture of [19] designed for such setups. Fig. 8b considers a Poisson channel, where \mathbf{x} is related to \mathbf{s} via a multivariate Poisson distribution, for which schemes requiring a linear Gaussian model such as the iterative SIC algorithm are not suitable. The ability of designing DNNs as neural building blocks to carry out their model-based algorithmic counterparts in a robust and model-agnostic fashion is demonstrated in Fig. 8. In particular, it

is demonstrated that DeepSIC approaches the SER values of the iterative SIC algorithm in linear Gaussian channels, while notably outperforming it in the presence of model mismatch, as well as when applied in non-Gaussian setups. It is also observed in Fig. 8a that the resulting architecture of DeepSIC can be trained with smaller data sets compared to alternative data-driven receivers, such as DetNet of [19], which is based on unfolding the projected gradient descent optimization method for MIMO detection.

Discussion: The main rationale in designing DNNs as interconnected neural building blocks is to facilitate learned inference by preserving the structured operation of a model-based algorithm applicable for the problem at hand given full domain knowledge. As discussed earlier, this approach can be treated as an extension of deep unfolding, allowing to exploit additional structures beyond a sequential iterative operation. For instance, DeepSIC designs its building-block DNNs to be interconnected in both parallel as well as a sequential manner. Nonetheless, the generalization of deep unfolding into a set of learned building blocks opens additional possibilities in designing model-aided networks.

First, the treatment of the model-based algorithm as a set of building blocks with concrete tasks allows a DNN architecture designed to comply with this structure not only to learn to carry out the original model-based method from data, but also to robustify it and enable its application in diverse new scenarios. This follows since the block diagram structure of the algorithm may be ignorant of the specific underlying statistical model, and only rely upon a set of generic assumptions, e.g., that the entries of the desired vector s are mutually independent. Consequently, replacing these building blocks with dedicated DNNs allows to exploit their model-agnostic nature, and thus the original algorithm can now be learned to be carried out in complex environments. For instance, DeepSIC can be applied to non linear channels, owing to the implementation of the building blocks of the iterative SIC algorithm using generic DNNs, while the model-based algorithm is limited to setups of the form (14) where the contribution of the interference is additive and can be canceled by subtraction.

In addition, the division into building blocks gives rise to the possibility to train each block separately. The main advantage in doing so is that a smaller training set is expected to be required, though in the horizon of a sufficiently large amount of training, end-to-end training is likely to yield a more accurate model as its parameters are jointly optimized. For example, in DeepSIC, sequential training uses the n_t input-output pairs to train each DNN individually. Compared to the end-to-end training that utilizes the training samples to learn the complete set of parameters, which can be quite large, sequential training uses the same data set to learn a significantly smaller number of parameters, reduced by a factor of $K \cdot Q$, multiple times. This indicates that the ability to train the blocks individually is expected to require much fewer training samples, at the cost of a longer learning procedure for a given training set, due to its sequential operation, and possible performance degradation as the building blocks are not jointly trained.

V. DNN-AIDED INFERENCE

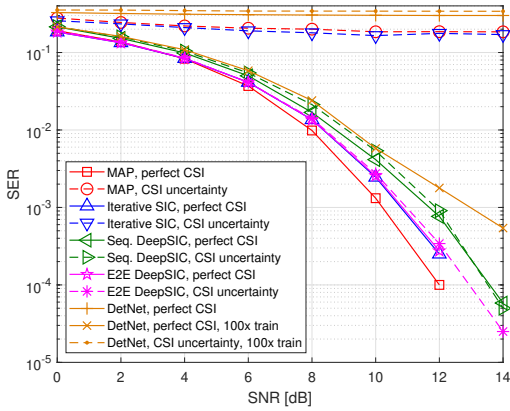
DNN-aided inference is a family of model-based deep learning algorithms in which DNNs are incorporated into model-based methods. As opposed to the model-aided networks strategy discussed in Section IV, where the resultant inference system is a deep network whose architecture imitates the operation of a model-based algorithm, here inference is carried out using a traditional model-based method, while some of the intermediate computations are empowered by DNNs. An illustration of a DNN-aided inference system obtained by integrating deep learning into a model-based algorithm is depicted in Fig. 9.

The main motivation for designing DNN-aided inference is to exploit the established benefits of model-based methods, in terms of performance, complexity, and suitability for the problem at hand, while using deep learning to empower the original algorithm. Such empowerment can correspond to mitigating sensitivity to inaccurate model knowledge, facilitating operation in complex environments, and enabling application of the algorithm in new domains.

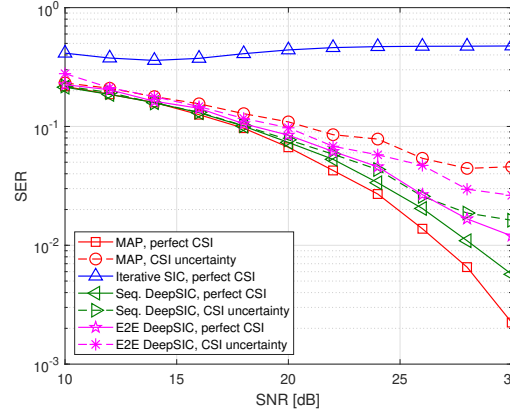
DNN-aided inference is particularly suitable for scenarios in which one only has access to partial domain knowledge. In such cases, the available domain knowledge dictates the algorithm utilized, while the part that is not available or is too complex to model analytically is tackled using deep learning. We divide our description of DNN-aided inference schemes into three main families of methods: The first, referred to as *structure-agnostic DNN-aided inference* detailed in Subsection V-A, utilizes deep learning to capture structures in the underlying data distribution, e.g., to represent the domain of natural images. This DNN is then utilized by model-based methods for the problem at hand, e.g., image reconstruction, allowing them to operate in a manner which is invariant to these structures. The family of *structure-oriented DNN-aided inference* schemes, detailed in Subsection V-B, utilizes model-based algorithms to exploit a known tractable statistical structure, such as an underlying Markovian behavior of the considered signals. In such methods, deep learning is incorporated into the structure-aware algorithm, thereby capturing the remaining portions of the underlying model as well as mitigating sensitivity to uncertainty. Finally, in Subsection V-C, we discuss *neural augmentation* methods, which are tailored to robustify model-based processing in the presence of inaccurate knowledge of the parameters of the underlying model. Here, inference is carried out using a model-based algorithm based on its available domain knowledge, while a deep learning system operating in parallel is utilized to compensate for errors induced by model inaccuracy.

A. Structure-Agnostic DNN-Aided Inference

The first family of DNN-aided inference utilizes deep learning to implicitly learn structures and statistical properties of the signal of interest, in a manner that is amenable to model-based optimization. These structure-agnostic hybrid model-based/data-driven inference systems are particularly relevant for various inverse problems in signal processing, including denoising, sparse recovery, deconvolution, and super resolution [22]. Tackling such problems typically involves imposing



(a) 32×32 Gaussian channel.



(b) 4×4 Poisson channel.

Fig. 8: Experimental results from [17] of DeepSIC compared to the model-based iterative SIC, the model-based MAP (when feasible) and the data-driven DetNet of [19] (when applicable). *Perfect CSI* implies that the system is trained and tested using samples from the same channel, while under *CSI uncertainty* they are trained using samples from a set of different channels.

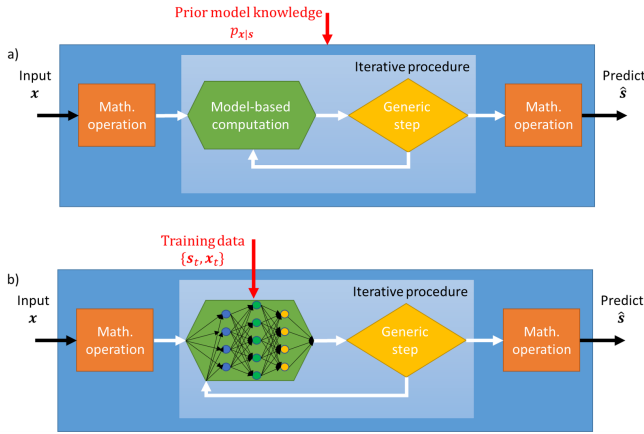


Fig. 9: DNN-aided inference illustration: *a)* a model-based algorithm comprised of multiple iterations with intermediate model-based computations; *b)* A data-driven implementation of the algorithm, where the specific model-based computations are replaced with dedicated learned deep models.

some structure on the target signal. This prior knowledge is then incorporated into a model-based optimization procedure, such as the alternating direction method of multipliers [59], the fast iterative shrinkage and thresholding algorithm [54], and primal-dual splitting [60], which recover the desired signal with provable performance guarantees.

Traditionally, the prior knowledge encapsulating the structure and properties of the underlying signal is represented by a handcrafted regularization term or constraint incorporated into the optimization objective. For example, a common model-based strategy used in various inverse problems is to impose sparsity in some given dictionary [26], which facilitates CS-based optimization. Deep learning brings forth the possibility to avoid such explicit constraint, thereby mitigating the detrimental effects of crude, handcrafted approximation of the true underlying structure of the signal. In particular, structure-agnostic DNN aided inference builds upon the model-agnostic nature of deep learning and its ability to operate reliably

in complex and analytically intractable setups, to facilitate optimization with implicit data-driven regularization. This can be implemented by incorporating deep denoisers as learned proximal mappings in iterative optimization, as carried out by plug-and-play networks¹ [14], [15], [61]–[66]. DNN-based priors can also be used to enable, e.g., CS beyond the domain of sparse signals [10]–[12], as we review in the next example.

Design Outline: Structure-agnostic DNN-aided inference integrates deep learning into model-based optimization in order to faithfully capture complex signal domains without having to manually characterize them. The resulting hybrid model-based/data-driven systems thus carry out model-based optimization over analytically intractable domains. Designing structure-agnostic DNN-aided systems can be carried out via the following steps:

- 1) Identify the optimization procedure for the problem at hand, given the domain knowledge for the signal of interest.
- 2) The specific parts of the optimization procedure which rely on complicated and possibly analytically intractable domain knowledge are replaced with a DNN.
- 3) The integrated data-driven module can either be trained separately from the inference system, possibly in an unsupervised manner as in [10], or alternatively the complete inference system can be trained end-to-end [13].

We next demonstrate how these steps are carried out for CS over complicated domains, using the application of deep generative networks as deep priors [10].

Example: Compressed Sensing using Generative Models: CS refers to the task of recovering some unknown signal from (possibly noisy) lower-dimensional observations. The mapping that transforms the input signal to the observations is known as the *forward operator*. In our example, we focus on the setting

¹The term *plug-and-play* typically refers to the usage of an image denoiser as proximal mapping in regularized optimization [61]. As this approach can also utilize model-based denoisers, we use the term *plug-and-play networks* for such methods with DNN-based denoisers.

where the forward operator is a particular linear function that is known at the time of signal recovery.

The main challenge in CS is that there could be (potentially infinitely) many signals that agree with the given observations. Since such a problem is underdetermined, it is necessary to make some sort of structural assumption on the unknown signal to identify the most plausible one. A classic assumption is that the signal is *sparse* in some known basis.

a) *System Model*: We consider the problem of noisy CS, where we wish to reconstruct an unknown N -dimensional signal s^* from the following observations:

$$\mathbf{x} = \mathbf{A}\mathbf{s}^* + \mathbf{w}, \quad (19)$$

where \mathbf{A} is an $M \times N$ matrix, modeled as random Gaussian matrix with entries $A_{ij} \sim \mathcal{N}(0, 1/M)$, with $M < N$, and \mathbf{w} is an $M \times 1$ noise vector.

b) *Sparsity-based CS*: Here we focus on a particular technique as a representative example of model-based CS [26]. We rely here on the assumption that s^* is sparse, e.g., $\|s^*\|_0 = l$ with $l \ll N$. More generally, it may be sparse in an appropriate representation. Our goal is to find the sparsest s that agrees with the noisy observations:

$$\begin{aligned} & \text{minimize } \|s\|_0 \\ & \text{subject to } \|\mathbf{A}s - \mathbf{x}\|_2 \leq \epsilon, \end{aligned}$$

where ϵ is a noise threshold. Although the above ℓ_0 norm optimization problem is NP-hard, [67], [68] showed that it suffices to minimize the following ℓ_1 relaxation, referred to as the LASSO objective:

$$\mathcal{L}_{\text{LASSO}}(s) \triangleq \|\mathbf{A}s - \mathbf{x}\|_2^2 + \lambda \|s\|_1 \quad (20)$$

The formulation (20) is convex, and for Gaussian \mathbf{A} with $l = \|s^*\|_0$ and $m = \Theta(l \log \frac{n}{l})$, the unique minimizer of $\mathcal{L}_{\text{LASSO}}$ is equal to s^* with high probability.

c) *DNN-Aided Compressed Sensing*: In a data-driven approach, we aim to replace the sparsity prior with a learned DNN. The following description is based on [10], which proposed to use a deep generative prior. Specifically, we replace the explicit sparsity assumption on true signal s^* , with a requirement that it lies in the range of a pre-trained generator network $G: \mathbb{R}^l \rightarrow \mathbb{R}^N$ (e.g. the generator network of a GAN).

Pre-training: To implement deep generative priors, one first has to train a generative network G to map a latent vector z from an i.i.d. Gaussian distribution into a signal s which lies in the domain of interest. A major advantage of employing a DNN-based prior in this setting is that generator networks are agnostic to how they are used and can be *pre-trained* and reused for multiple downstream tasks. The pre-training thus follows the standard unsupervised training procedure, as discussed, e.g., in Subsection III-B for GANs. In particular, the work [10] trained a DCGAN [69], a particular type of GAN designed to work well with image data, on the CelebA data set [70], to represent 64×64 color images of human faces, as well as a VAE [38] for representing handwritten digits in 28×28 grayscale form based on the MNIST data set [71].

Architecture: Once a pre-trained generator network $G: z \mapsto s$ is available, it can be incorporated as an alternative

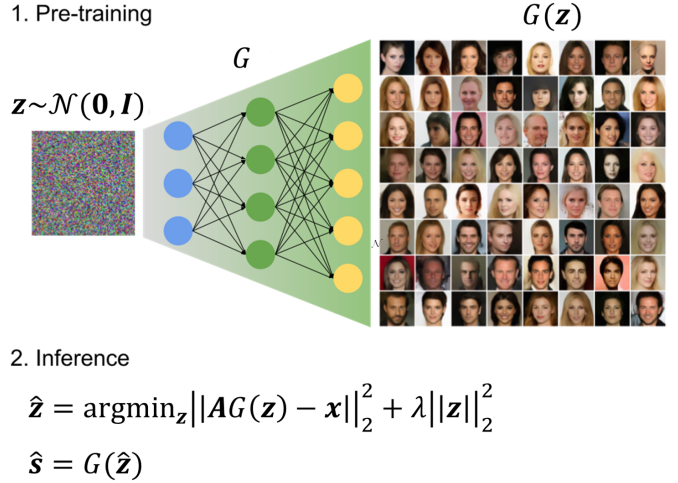


Fig. 10: High-level overview of compressed sensing with a DNN-based prior. The generator network G is pre-trained to map Gaussian latent variables to plausible signals in the target domain. Then the signal recovery is done by finding a point in the range of G that minimizes reconstruction error (with an appropriate regularization term as shown) via gradient-based optimization over the latent variable.

prior for the inverse model in (19). The key intuition behind this approach is that the range of G should only contain *plausible* signals. Thus one can replace the handcrafted sparsity prior with a data-driven DNN prior G by constraining our signal recovery to the range of G .

One natural way to impose this constraint is to perform the optimization in the latent space to find z whose image $G(z)$ matches the observations. This is carried out by minimizing the following loss function in the latent space of G :

$$\mathcal{L}(z) = \|\mathbf{A}G(z) - \mathbf{x}\|_2^2. \quad (21)$$

Because the above loss function involves a highly non-convex function G , there is no closed-form solution or guarantee for this optimization problem. However the loss function is differentiable with respect to z , so it can be tackled using gradient-based optimization techniques such as Adam [33] mentioned in Section III. Once a suitable latent variable z is found, the actual signal we return is $G(z)$.

In practice, [10] reports that incorporating an ℓ_2 regularizer on z helps. This is possibly due to the Gaussian prior assumption for the latent variable, as the density of z is proportional to $\exp(-\|z\|_2^2)$. Therefore, minimizing $\|z\|_2^2$ is equivalent to maximizing the density of z under the Gaussian prior. This has the effect of avoiding images that are extremely unlikely under the Gaussian prior even if it matches the observation well. The final loss includes this regularization term:

$$\mathcal{L}_{\text{CS}}(z) = \|\mathbf{A}G(z) - \mathbf{x}\|_2^2 + \lambda \|z\|_2^2, \quad (22)$$

where λ is a hyperparameter that controls the strength of the regularization.

In summary, DNN-aided CS replaces the constrained optimization over the complex input signal with tractable optimization over the latent variable z , which follows a known simple distribution, using a pre-trained DNN-based prior G to

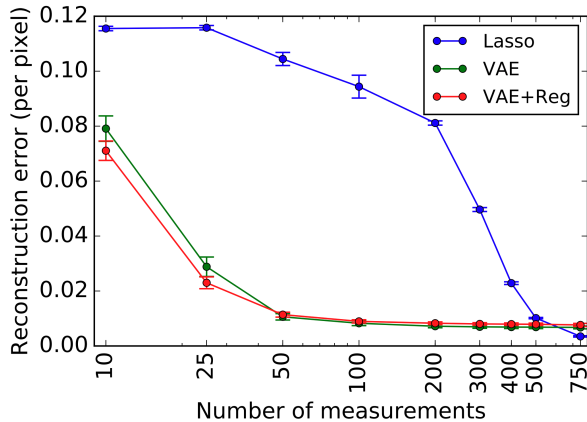


Fig. 11: Experimental result for noisy CS on the MNIST data set. Reproduced from [10] with the authors’ permission.

map it into the domain of interest. Inference is performed by minimizing \mathcal{L}_{CS} in the latent space of G through a gradient-based optimization. An illustration of the system operation is depicted in Fig. 10.

Quantitative Results: To showcase the efficacy of the data-driven prior at capturing complex high-dimensional signal domains, we present the evaluation of its performance in recovering MNIST and CelebA images from lower-dimensional projections, as reported in [10]. The baseline model used for comparison is based on directly solving the LASSO loss (20). For CelebA, we formulate the LASSO objective in the discrete cosine transform (DCT) and the wavelet (WWT) basis, and minimize it via coordinate descent.

The first task is the recovery of handwritten digit images from low-dimensional projections corrupted by additive Gaussian noise $w \sim \mathcal{N}(\mathbf{0}, \sigma^2 \mathbf{I}_M)$ where $\sigma = 0.1$. The unknown signal to be recovered is chosen from the test set, previously unseen to the generator G during training. The reconstruction error is evaluated for various numbers of observations M . The results are depicted in Fig. 11.

We clearly see the benefit of using a data-driven deep prior in Fig. 11, where the VAE-based methods (labeled VAE and VAE+REG) show remarkable performance gain compared to the sparsity prior for small number of measurements. Implicitly imposing a sparsity prior via the Lasso objective outperforms the deep generative priors as the number of observations approaches the dimension of the signal. One explanation for this behavior is that the pre-trained generator G does not perfectly model the MNIST digit distribution and may not actually contain the ground truth signal in its range. As such, its reconstruction error may never be exactly zero regardless of how many observations are given. The LASSO objective, on the other hand, does not suffer from this issue and is able to make use of the extra observations available.

The ability of deep generative priors to facilitate recovery from compressed measurements is also observed in Fig. 12, which qualitatively evaluates the performance of GAN-based CS recovery on the CelebA dataset. For this experiment, we use $M = 500$ measurements (out of $N = 12288$ total dimensions) again with Gaussian noise $w \sim \mathcal{N}(\mathbf{0}, \sigma^2 \mathbf{I}_M)$ where $\sigma = 0.01$. As shown in Fig. 12, in this low-measurement

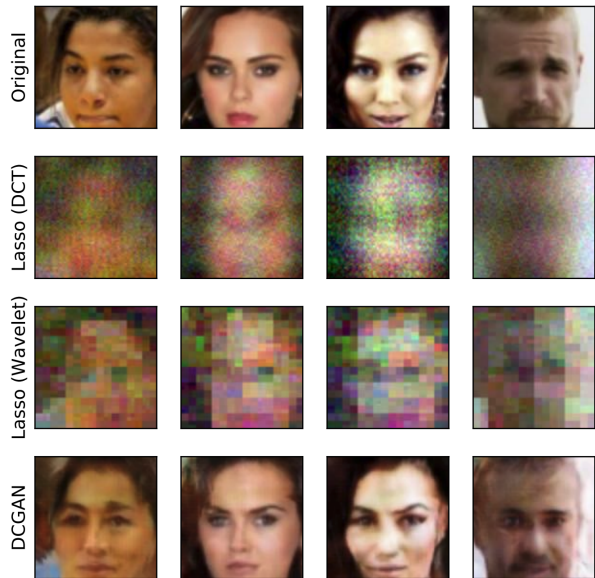


Fig. 12: Visualization of the recovered signals from noisy CS on the CelebA data set. Reproduced from [10] with the authors’ permission.

regime, the data-driven prior again provides much more reasonable samples.

Discussion: Using deep learning to empower regularized optimization builds upon the model-agnostic nature of DNNs. Traditional optimization methods rely on mathematical expressions to capture the structure of the solution one is looking for, inevitably inducing model mismatch in domains which are extremely challenging to describe analytically. The ability of deep learning to learn complex mappings without relying on domain knowledge is exploited here to bypass the need for explicit regularization. This application of DNNs can take the form of deep priors, where the domain of interest is captured by a generative network, as detailed in the above example. An alternative strategy is to apply deep denoisers as learned proximal mappings, as done in plug-and-play networks [61]. This approach avoids the need to mathematically formulate a proximal operator which faithfully matches the problem at hand, while relying on the qualities of established DNN denoisers, such as DnCNN [72].

The fact that structure-agnostic DNN-aided inference utilizes deep learning to capture the domain of interest facilitates using pre-trained networks. This property reduces the dependency of the system on massive amounts of labeled data. For instance, the usage of deep generative priors is based on DNN architectures which are trained in an unsupervised manner, and thus relies only on unlabeled data, e.g., natural images. Such unlabeled samples are typically more accessible and easy to aggregate compared to labeled data, e.g., tagged natural images. One can often utilize off-the-shelf pre-trained DNNs when such network exist for domains related to the ones over which optimization is carried out, with possible adjustments to account for the subtleties of the problem by transfer learning.

Finally, while our description of DNN-empowered regularized optimization relies on model-based iterative optimizers which utilize a deep learning module, one can also incorporate

deep learning into the optimization procedure. For instance, the iterative optimization steps can be unfolded into a DNN, as in, e.g., [73]. This approach allows to benefit from both the ability of deep learning to implicitly represent complex domains, as well as the inference speed reduction of deep unfolding along with its robustness to uncertainty and errors in the model parameters assumed to be known. Nonetheless, the fact that the iterative optimization must be learned from data in addition to the structure of the domain of interest implies that larger amounts of labeled data are required to train the system, compared to using the model-based optimizer.

B. Structure-Oriented DNN-Aided Inference

The family of structure-oriented DNN-aided inference algorithms utilize model-based methods designed to exploit an underlying statistical structure, while integrating DNNs to enable operation without additional explicit characterization of this model. The types of structures exploited in the literature can come in the form of an a-priori known factorizable distribution, such as causality and finite memory in communication channels [16], [18], [74]; it can follow from an established approximation of the statistical behavior, such as modelling of images as conditional random fields [75]–[77]; follow from physical knowledge of the system operation [78]; or arise due to the distributed nature of the problem, as in [79].

The main advantage in accounting for such statistical structures stems from the availability of various model-based methods, tailored specifically to exploit these structures, in order to facilitate accurate inference at reduced complexity. Many of these algorithms, such as the Kalman filter and its variants [80, Ch. 7], which build upon an underlying state-space structure, or the Viterbi algorithm [81], which exploits the presence of a hidden Markov model, can be represented as special cases of the broad family of factor graph methods. Consequently, our main example used for describing structure-oriented DNN-aided inference focuses on the implementation of message passing over data-driven factor graphs, which encapsulate factorizable distributions.

Design Outline: Structure-oriented DNN-aided algorithms exploit domain knowledge of statistical structures to carry out model-based inference methods in a data-driven fashion. These hybrid systems thus utilize deep learning not for the overall inference task, but for robustifying and relaxing the model-dependence of established model-based inference algorithms designed specifically for the structure induced by the specific problem being solved. The design of such DNN-aided hybrid inference systems consists of the following steps:

- 1) A proper inference algorithm is chosen based on the available knowledge of the underlying statistical structure. The domain knowledge is encapsulated in the selection of the algorithm which is learned from data. For example, when the underlying distribution is known to take a factorizable form, accurate inference at linear complexity can be obtained by applying the sum-product (SP) algorithm over a factor graph representation of the distribution.
- 2) Once a model-based algorithm is selected, we identify its model-specific computations, and replace them with dedicated compact DNNs.

- 3) The resulting DNNs are either trained individually, or the overall system can be trained in an end-to-end manner.

We next demonstrate how these steps are translated in a hybrid model-based/data-driven algorithm, using the learned factor graph inference for Markovian sequences proposed in [82] as an example.

Example: Learned Factor Graphs: Factor graph methods, such as the SP algorithm, exploit the factorization of a joint distribution to efficiently compute a desired quantity [83]. In particular, the application of the SP algorithm for distributions which can be represented as non-cyclic factor graphs, such as Markovian models, allows computing the MAP rule, an operation whose burden typically grows exponentially with the label space dimensionality, with complexity that only grows linearly with it. While the following description focuses on Markovian stationary time sequences, it can be extended to various forms of factorizable distributions.

a) *System Model:* We consider the problem of recovering a desired time series $\{s_i\}$ taking values in a finite set \mathcal{S} from an observed sequence $\{x_i\}$ taking values in a set \mathcal{Y} . The subscript i denotes the time index. The joint distribution of $\{s_i\}$ and $\{x_i\}$ obeys an l th-order Markovian stationary model, $l \geq 1$, and particularly

$$p(x_i, s_i | \{x_j, s_j\}_{j < i}) = p(x_i | s_{i-l}^i) p(s_i | s_{i-l}^{i-1}). \quad (23)$$

Consequently, when the initial state $\{s_i\}_{i=-l}^0$ is given, the joint distribution of $\mathbf{x} = [x_1, \dots, x_t]^T$ and $\mathbf{s} = [s_1, \dots, s_t]^T$ satisfies

$$p(\mathbf{x}, \mathbf{s}) = \prod_{i=1}^t p(x_i | s_{i-l}^i) p(s_i | s_{i-l}^{i-1}), \quad (24)$$

for any fixed sequence length $t > 0$, where we write $s_i^j \triangleq [s_i, s_{i+1}, \dots, s_j]^T$ for $i < j$.

b) *The Sum-Product Algorithm:* When the joint distribution of \mathbf{s} and \mathbf{x} is a-priori known and can be computed, the inference rule that minimizes the error probability for each time instance is the MAP detector,

$$\hat{s}_i(\mathbf{x}) = \arg \max_{s_i \in \mathcal{S}} p(s_i | \mathbf{x}), \quad (25)$$

for each $i \in \{1, \dots, t\} \triangleq \mathcal{T}$. This rule can be efficiently approached for finite-memory distributions using the SP algorithm [83].

To formulate the SP method, the factorizable distribution (24) is first represented as a factor graph. To that aim, define the vector variable $\mathbf{s}_i \triangleq s_{i-l+1}^i \in \mathcal{S}^l$, and the function

$$f(x_i, \mathbf{s}_i, \mathbf{s}_{i-1}) \triangleq p(x_i | \mathbf{s}_i, \mathbf{s}_{i-1}) p(\mathbf{s}_i | \mathbf{s}_{i-1}). \quad (26)$$

Note that when \mathbf{s}_i is a shifted version of \mathbf{s}_{i-1} , (26) coincides with $p(x_i | s_{i-l}^i) p(s_i | s_{i-l}^{i-1})$, and that it equals zero otherwise. Using (26), the joint distribution $p(\mathbf{x}, \mathbf{s})$ in (24) can be written as

$$p(\mathbf{x}, \mathbf{s}) = \prod_{i=1}^t f(x_i, \mathbf{s}_i, \mathbf{s}_{i-1}). \quad (27)$$

The factorizable expression of the joint distribution (27) implies that it can be represented as a factor graph with t function

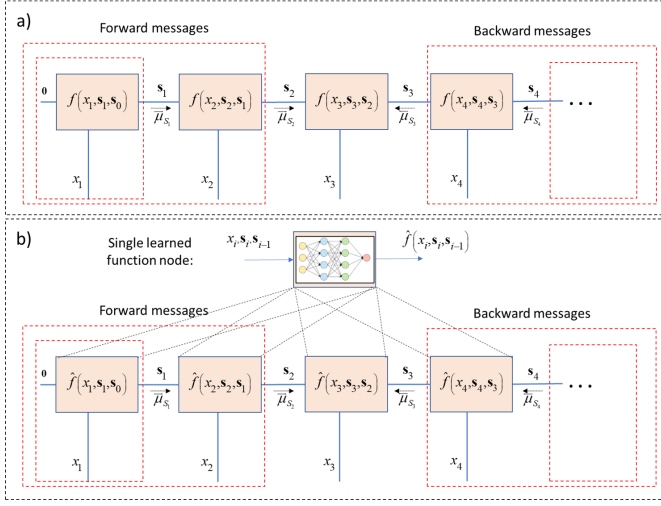


Fig. 13: Illustration of the SP method for Markovian sequences using a) the true factor graph; and b) a learned factor graph.

nodes $\{f(x_i, \mathbf{s}_i, \mathbf{s}_{i-1})\}$, in which $\{\mathbf{s}_i\}_{i=2}^{t-1}$ are edges while the remaining variables are half-edges.

Using its factor graph representation, one can compute the joint distribution of \mathbf{s} and \mathbf{x} by recursive message passing along its factor graph. In particular,

$$p(\mathbf{s}_k, \mathbf{s}_{k+1}, \mathbf{x}) = \vec{\mu}_{\mathbf{s}_k}(\mathbf{s}_k) f(x_{k+1}, \mathbf{s}_{k+1}, \mathbf{s}_k) \overleftarrow{\mu}_{\mathbf{s}_{k+1}}(\mathbf{s}_{k+1}), \quad (28)$$

where the forward path messages satisfy

$$\vec{\mu}_{\mathbf{s}_i}(\mathbf{s}_i) = \sum_{\mathbf{s}_{i-1}} f(x_i, \mathbf{s}_i, \mathbf{s}_{i-1}) \vec{\mu}_{\mathbf{s}_{i-1}}(\mathbf{s}_{i-1}), \quad (29)$$

for $i = 1, 2, \dots, k$. Similarly, the backward messages are

$$\overleftarrow{\mu}_{\mathbf{s}_i}(\mathbf{s}_i) = \sum_{\mathbf{s}_{i+1}} f(x_{i+1}, \mathbf{s}_{i+1}, \mathbf{s}_i) \overleftarrow{\mu}_{\mathbf{s}_{i+1}}(\mathbf{s}_{i+1}), \quad (30)$$

for $i = t-1, t-2, \dots, k+1$. This message passing is illustrated in Fig. 13(a).

The ability to compute the joint distribution in (28) via message passing allows to obtain the MAP detector in (25) with complexity that only grows linearly with t . This is achieved by noting that the MAP estimate satisfies

$$\hat{\mathbf{s}}_i(\mathbf{x}) = \arg \max_{\mathbf{s}_i \in \mathcal{S}} \sum_{\mathbf{s}_{i-1} \in \mathcal{S}^l} \vec{\mu}_{\mathbf{s}_{i-1}}(\mathbf{s}_{i-1}) f(x_i, [\mathbf{s}_{i-l+1}, \dots, \mathbf{s}_i], \mathbf{s}_{i-1}) \times \overleftarrow{\mu}_{\mathbf{s}_i}([\mathbf{s}_{i-l+1}, \dots, \mathbf{s}_i]), \quad (31)$$

for each $i \in \mathcal{T}$, where the summands can be computed recursively. When the block size t is large, the messages may tend to zero, and are thus commonly scaled [84], e.g., $\overleftarrow{\mu}_{\mathbf{s}_i}(\mathbf{s})$ is replaced with $\gamma_i \overleftarrow{\mu}_{\mathbf{s}_i}(\mathbf{s})$ for some scale factor which does not depend on \mathbf{s} , and thus does not affect the MAP rule.

c) *Learned Factor Graphs*: Learned factor graphs enable learning to implement MAP detection from labeled data. It utilizes the a-priori known factorization to determine the structure of the factor graph, while using deep learning to compute the function nodes without having to explicitly specify their computations. Finally, it carries out the SP method for inference over the resulting learned factor graph.

Architecture: In order to implement the SP algorithm, one must be able to specify the factor graph representing

the underlying distribution. Learned factor graphs combine domain knowledge with deep learning to obtain this graphical representation. In particular, the stationarity assumption implies that the complete factor graph is encapsulated in the single function $f(\cdot)$ (26) regardless of the block size t . Building upon this insight, DNNs can be utilized to learn the mapping carried out at the function node separately from the inference task. The resulting learned stationary factor graph is then used to recover $\{\mathbf{s}_i\}$ by message passing, as illustrated in Fig. 13(b). As learning a single function node is expected to be a simpler task compared to learning the overall inference method for recovering \mathbf{s} from \mathbf{x} , this approach allows using relatively compact DNNs, which in turn can be learned from a relatively small set of labeled data. Furthermore, the learned function node describes the factor graph for different values of t . When the learned function node, denoted $\hat{f}_\theta(\cdot)$, is an accurate estimate of the true one, the MAP detection rule (25) is effectively implemented, and thus the inference performance approaches the minimal probability of error.

Training: The function node which encapsulates the factor graph of stationary finite-memory channels is given in (26). In order to learn a stationary factor graph from samples, one must only learn its function node, which here boils down to learning $p(x_i | \mathbf{s}_{i-1}^{i-1})$ and $p(\mathbf{s}_i | \mathbf{s}_{i-1}^{i-1})$ by (26). Specifically, for stationary sequences, only a single function node must be learned, as the mapping $f(\cdot)$ does not depend on the time index i . When $\{\mathbf{s}_i\}$ take values in a finite set, i.e., \mathcal{S} is finite, the transition probability $p(\mathbf{s}_i | \mathbf{s}_{i-1}^{i-1})$ can be learned via a histogram.

For learning the distribution $p(x_i | \mathbf{s}_{i-1}^{i-1})$, it is noted that

$$p(x_i | \mathbf{s}_i) = p(\mathbf{s}_i | x_i) p(x_i) (p(\mathbf{s}_i))^{-1}. \quad (32)$$

A parametric estimate of $p(\mathbf{s}_i | x_i)$, denoted $\hat{P}_\theta(\mathbf{s}_i | x_i)$, is obtained for each $\mathbf{s}_i \in \mathcal{S}^{l+1}$ by training classification networks with softmax output layers to minimize the cross entropy loss. As the SP mapping is invariant to scaling $f(x_i, \mathbf{s}_i, \mathbf{s}_{i-1})$ with some factor which does not depend on the $\mathbf{s}_i, \mathbf{s}_{i-1}$, one can set $p(x_i) \equiv 1$ in (32), and use the result to obtain a scaled value of the function node, which, as discussed above, does not affect the inference mapping.

Quantitative Results: As a numerical example of learned factor graphs for Markovian models, we consider a scenario of symbol detection over causal stationary communication channels with finite memory, reproduced from [82]. Fig. 14 depicts the numerically evaluated SER achieved by applying the SP algorithm over a factor graph learned from $n_t = 5000$ labeled samples, for channels with memory $l = 4$. The results are compared to the performance of the model-based SP methods, which requires complete knowledge of the underlying statistical model, as well as the sliding bidirectional RNN detector proposed in [85] for such setups, which utilizes a conventional DNN architecture that does not explicitly account for the Markovian structure. In particular, Fig. 14a considers a Gaussian channel, while in Fig. 14b the conditional distribution $p(x_i | \mathbf{s}_{i-1}^{i-1})$ represents a Poisson distribution. Fig. 14 demonstrates the ability of learned factor graphs to enable accurate message passing inference in a data-driven manner, as the performance achieved using learned factor graphs

approaches that of the SP algorithm, which operates with full knowledge of the underlying statistical model. The numerical results also demonstrate that combining model-agnostic DNNs with model-aware inference notably improves robustness to model uncertainty compared to applying the SP algorithm with the inaccurate model. Furthermore, it is also observed that explicitly accounting for the Markovian structure allows to achieve improved performance compared to utilizing black-box DNN architectures such as the sliding bidirectional RNN detector, with limited data sets for training.

Discussion: The integration of deep learning into structure-oriented model-based algorithms allows to exploit the model-agnostic nature of DNNs while explicitly accounting for available structural domain knowledge. Consequently, structure-oriented DNN-aided inference is most suitable for setups in which structured domain knowledge naturally follows from the underlying physics or from established models of the problem, while the subtleties of the complete statistical knowledge may be challenging to accurately capture analytically. Such structural knowledge is often present in various problems in signal processing and communications. For instance, modelling communication channels as causal finite-memory systems, as assumed in the above quantitative example, is a well-established representation of many physical channels, regardless of the specific characteristics of the setup and the communicating devices. Another example is state-space models, which are widely-used in control scenarios. State-space models represent transitions of an unknown state in a structured manner, while the unique properties of the problem at hand are encapsulated in the equations describing the state evolution and corresponding measurements. The availability of established structures in signal processing related setups, makes structure-oriented DNN-aided inference a candidate approach to facilitate inference in such scenarios in a manner which is ignorant of the unique and possibly intractable subtleties of the problem, by learning to account for them implicitly from data.

Structure-oriented DNN-aided inference, in which deep learning is used to learn an intermediate model-based computation rather than the complete predication rule, facilitates the usage of relatively compact DNNs. This property implies that the resulting system can be trained using scarce data sets. One can exploit the fact that the system can be trained using small training sets to, e.g., enable online adaptation to temporal variations in the underlying statistical model based on some future feedback on the correctness of the inference rule. This property was exploited in [16] to facilitate online training of DNN-aided receivers in coded communications. Furthermore, while structure-oriented DNN-aided systems are geared towards exploiting statistical structures, this approach can also incorporate additional forms of domain knowledge. For instance, the learned factor graphs example presented above utilize prior knowledge of an underlying stationarity to substantially reduce the number of learned parameters, capturing the complete learned factor graph in a single learned function node.

A DNN integrated into a structure-oriented model-based inference method, such as the SP algorithm, can be either

trained individually, i.e., independently of the inference task, or in an end-to-end fashion. The first approach typically requires less training data, and the resulting trained DNN can be combined with various inference algorithms. For instance, the learned function node used to carry out SP inference in the above example can also be integrated into the Viterbi algorithm as done in [16], which can be treated as message passing with forward messages and thus predicts in real time. Alternatively, the learned modules can be tuned in an end-to-end fashion by formulating their objective as that of the overall inference algorithm, and backpropagating through the model-based computations, see, e.g., [77]. Learning in an end-to-end fashion facilitates overcoming inaccuracies in the assumed structures, possibly by incorporating learned methods to replace the generic computations of the model-based algorithm, at the cost of requiring larger volumes of data for training purposes.

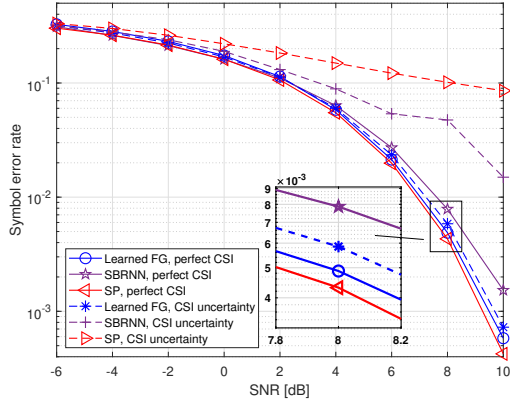
C. Neural Augmentation

The DNN-aided inference strategies detailed in Subsections V-A and V-B utilize model-based algorithms to carry out inference, while replacing explicit domain-specific computations with dedicated DNNs. An alternative approach, referred to as *neural augmentation*, utilizes the complete model-based algorithm for inference, i.e., without embedding deep learning into its components, while using an external DNN for correcting some of its intermediate computations [20], [21], [86]. An illustration of this approach is depicted in Fig. 15.

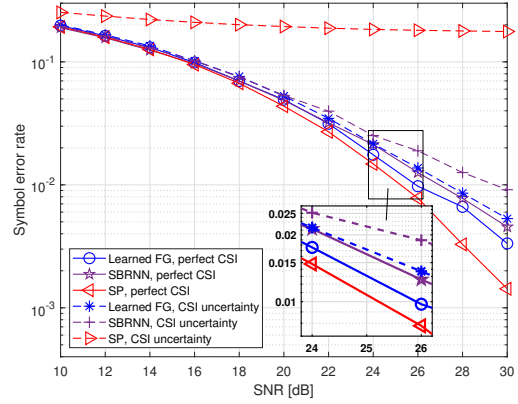
The main advantage in utilizing an external DNN for correcting internal computations of a model-based algorithm follows from its ability to notably improve the robustness of model-based methods to inaccurate knowledge of the underlying model parameters. Since the model-based algorithm is individually implemented, one must possess the complete domain knowledge it requires, and thus the external correction DNN allows the resulting hybrid model-based/data-driven system to overcome inaccuracies in this domain knowledge by learning to correct them from data. Furthermore, the learned correction term incorporated by neural augmentation can improve the performance of model-based algorithms in scenarios where they are known to be sub-optimal, as detailed in the example in the sequel.

Design Outline: Neural augmentation is based on adding an external learned correction module to an iterative model-based optimization method, whose purpose is to provide a correction term to the information exchanged between the iterations of the algorithm. The design of neural-augmented inference systems is comprised of the following steps:

- 1) Identify a suitable iterative optimization algorithm for the problem of interest. In particular, identify the information exchanged between the iterations, and the intermediate model-based computations which are used to produce this information.
- 2) The information exchanged between the iterations is updated with a correction term learned by a DNN. The DNN architecture is designed to combine the same quantities used by the model-based algorithm, only in a learned fashion.



(a) Gaussian channel.



(b) Poisson channel.

Fig. 14: Experimental results from [82] of learned factor graphs (Learned FG) compared to the model-based SP algorithm and the data-driven sliding bidirectional RNN (SBRNN) of [85]. *Perfect CSI* implies that the system is trained and tested using samples from the same channel, while under *CSI uncertainty* they are trained using samples from a set of different channels.

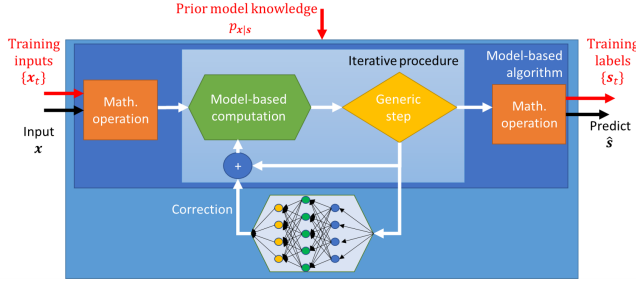


Fig. 15: Neural augmentation illustration.

- 3) The overall hybrid model-based/data-driven system is trained in an end-to-end fashion, where one can consider not only the algorithm outputs in the loss function, but also the intermediate outputs of the internal iterations.

We next demonstrate how these steps are carried out in order to empower Kalman smoothing via neural augmentation, as proposed in [86].

Example: Neural-Augmented Kalman Smoothing: The DNN-aided Kalman smoother proposed in [86] implements state estimation in environments characterized by state-space models. The integration of neural augmentation allows not only to robustly the Kalman smoother in the presence of inaccurate model knowledge, but also to improve its performance in non-linear setups, where variations of the Kalman algorithm, such as the extended Kalman method, are known to be sub-optimal [80, Ch. 7]. Therefore, while the description below considers linear state-space models, the quantitative example taken from [86] is taken from a non-linear case.

a) System Model: Consider a linear Gaussian state-space model. Here, one is interested in recovering a sequence of t continuous state RVs $\{s_i\}_{i=1}^t$ from an observed sequence $\{x_i\}_{i=1}^t$. The observations are related to the desired state sequence via

$$x_i = H s_i + r_i, \quad (33a)$$

while the state transition takes the form

$$s_i = F s_{i-1} + w_i. \quad (33b)$$

In (33), r_i and w_i obey an i.i.d. zero-mean Gaussian distributions with covariance R and W , respectively, while H and F represent known linear mappings.

We focus on scenarios where the state-space model in (33), which is available to the inference system, is an inaccurate approximation of the true underlying dynamics. For such scenarios, one can apply Kalman smoothing, which is known to achieve minimal MSE recovery when (33) holds, while introducing a neural augmentation correction term [86].

b) Kalman Smoothing: The Kalman smoother computes the minimal MSE estimate of each s_i given a realization of $x = [x_1, \dots, x_t]^T$. Its procedure is comprised of forward and backward message passing, exploiting the Markovian structure of the state-space model to operate at complexity which only grows linearly with t . In particular, by writing $s = [s_1, \dots, s_t]^T$, one can approach the minimal MSE estimate by gradient descent optimization on the joint log likelihood function, i.e., by iterating over

$$s^{(q+1)} = s^{(q)} + \gamma \nabla_{s^{(q)}} \log p(x, s^{(q)}), \quad (34)$$

where $\gamma > 0$ is a step-size. The state-space model (33) implies that the i th entry of the log likelihood gradient in (34), abbreviated henceforth as $\nabla_i^{(q)}$, can be obtained as $\nabla_i^{(q)} = \mu_{s_{i-1} \rightarrow s_i}^{(q)} + \mu_{s_{i+1} \rightarrow s_i}^{(q)} + \mu_{x_i \rightarrow s_i}^{(q)}$, where the summands, referred to as messages, are given by

$$\mu_{s_{i-1} \rightarrow s_i}^{(q)} = -W^{-1} (s_i^{(q)} - F s_{i-1}^{(q)}), \quad (35a)$$

$$\mu_{s_{i+1} \rightarrow s_i}^{(q)} = F^T W^{-1} (s_{i+1}^{(q)} - F s_i^{(q)}), \quad (35b)$$

$$\mu_{x_i \rightarrow s_i}^{(q)} = H^T R^{-1} (x_i - F s_i^{(q)}). \quad (35c)$$

The iterative procedure in (34), is repeated until convergence, and the resulting $s^{(q)}$ is used as the estimate.

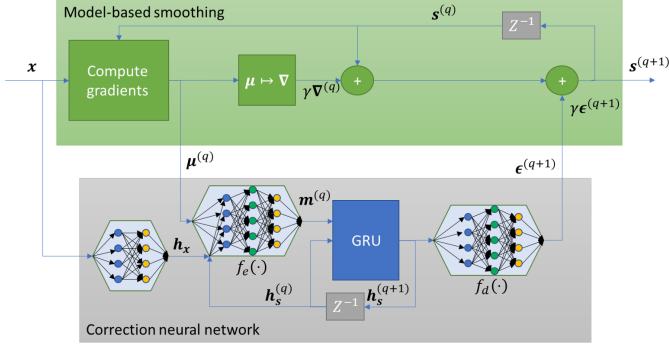


Fig. 16: Neural augmented Kalman smoother illustration. Blocks marked with Z^{-1} represent a single iteration delay.

c) *Neural-Augmented Kalman Smoothing*: The gradient descent formulation in (34) is evaluated by the messages (35), which in turn rely on accurate knowledge of the state-space model (33). Consequently, in order to facilitate operation in the presence of inaccurate model knowledge due to, e.g., (33) being a linear approximation of a non-linear setup, one can introduce neural augmentation to learn to correct inaccurate computations of the log-likelihood gradients. This is achieved by using an external DNN to map the messages in (35) into a correction term, denoted $\epsilon^{(q+1)}$.

Architecture: The learned mapping of the messages (33) into a correction term operates in the form of a graph neural network (GNN) [87]. This is implemented by maintaining an internal node variable for each variable in (35), denoted $h_{s_i}^{(q)}$ for each $s_i^{(q)}$ and h_{x_i} for each x_i , as well as internal message variables $m_{\mathbf{V}_n \rightarrow S_i}^{(q)}$ for each message computed by the model-based algorithm in (35). The node variables $h_{s_i}^{(q)}$ are updated along with the model-based smoothing algorithm iterations as estimates of their corresponding variables, while the variables h_{x_i} are obtained once from \mathbf{x} via a neural network. The GNN then maps the messages produced by the model-based Kalman smoother into its internal messages via a neural network $f_e(\cdot)$ which operates on the corresponding node variables, i.e.,

$$m_{\mathbf{V}_n \rightarrow S_i}^{(q)} = f_e \left(h_{\mathbf{v}_n}^{(q)}, h_{s_i}^{(q)}, \mu_{\mathbf{V}_n \rightarrow S_i}^{(q)} \right), \quad (36)$$

where $h_{x_n}^{(q)} \equiv h_{x_n}$ for each q . These messages are then combined and forwarded into a gated recurrent unit (GRU), which produces the refined estimate of the node variables $\{h_{s_i}^{(q+1)}\}$ based on their corresponding messages (36). Finally, each updated node variable $h_{s_i}^{(q+1)}$ is mapped into its corresponding error term $\epsilon_i^{(q+1)}$ via a fourth neural network, denoted $f_d(\cdot)$.

The correction terms $\{\epsilon_i^{(q+1)}\}$ aggregated into the vector $\epsilon^{(q+1)}$ are used by the model-based Kalman smoother to update the log-likelihood gradients, resulting in the update equation (34) replaced with

$$\mathbf{s}^{(q+1)} = \mathbf{s}^{(q)} + \gamma \left(\nabla_{\mathbf{s}^{(q)}} \log p \left(\mathbf{x}, \mathbf{s}^{(q)} \right) + \epsilon^{(q+1)} \right). \quad (37)$$

The overall architecture is illustrated in Fig. 16.

Training: Let θ be the overall parameters of the GNN in Fig. 16. The hybrid system is trained in an end-to-end manner to minimize the empirical weighted ℓ_2 norm loss over its intermediate layers, where the contribution of each iteration to

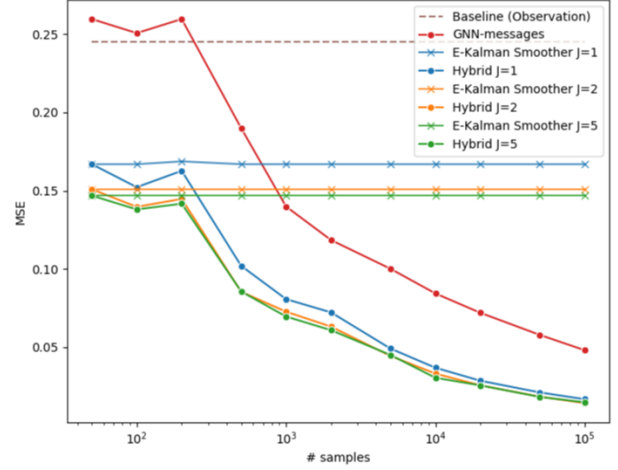


Fig. 17: MSE versus data set size for the Neural-augmented Kalman smoother (Hybrid) compared to the model-based extended Kalman smoother (E-Kalman) and a solely data-driven GNN, for various linearizations of state-space models (represented by the index j). Figure reproduced from [86] with authors' permission.

the overall loss increases as the iterative procedure progresses. In particular, by letting $\{s_t, \mathbf{x}_t\}_{t=1}^{n_t}$ denote the training set, the loss function used to train the neural-augmented Kalman smoother is given by

$$\mathcal{L}(\theta) = \frac{1}{n_t} \sum_{t=1}^{n_t} \sum_{q=1}^Q \frac{q}{Q} \|s_t - \hat{s}_q(x_t; \theta)\|^2, \quad (38)$$

where $\hat{s}_q(x_t; \theta)$ is the estimate produced by the q th iteration, i.e., via (37), with parameters θ and input x_t .

Quantitative Results: The experiment whose results are depicted in Fig. 17 considers a non-linear state-space model described by the Lorenz attractor equations, which describe atmospheric convection via continuous-time differential equations. Due to the non-linearity of the discrete-time state evolution, the model is linearized by approximating the non-linear dynamics with its j th order Taylor series expansion, and thus the state-space equations assumed by the model-based inference system constitute an approximation of the true dynamics.

Fig. 17 demonstrates the ability of neural augmentation to empower and improve model-based inference. It is observed that introducing the DNN-based correction term allows the system to learn to overcome the model inaccuracy, and achieve an error which decreases with the amount of available training data. It is also observed that the hybrid approach of combining model-based inference and deep learning enables accurate inference with notably reduced volumes of training data, as the individual application of the GNN for state estimation, which does not explicitly account for the available domain knowledge, requires much more training data to achieve similar accuracy as that of the neural-augmented Kalman smoother.

Discussion: Neural augmentation implements hybrid model-based/data-driven inference by utilizing two individual modules – a model-based algorithm and a DNN – with each capable of inferring on its own. For instance, the

neural-augmented Kalman smoother utilizes both an individual model-aware Kalman smoother which carries out inference, along with a GNN that can produce its own state estimates via its internal node variables. The rationale here is to benefit from both approaches by interleaving the iterative operation of the modules, and specifically by utilizing the data-driven component to learn to correct the model-based algorithm, rather than produce individual estimates. This approach thus conceptually differs from the previously discussed DNN-aided inference algorithms, where a DNN is integrated into a model-based algorithm and thus inference is achievable only by the combined efforts of the model-based and data-driven components.

The fact that neural augmentation utilizes individual model-based and data-driven modules reflects on its requirements and use cases. First, one must possess full domain knowledge, or at least an approximation of the true model, in order to implement model-based inference. For instance, the neural-augmented Kalman smoother required full knowledge of the state-space model (33), or at least an approximation of this analytical closed-form model as used in the quantitative example, in order to compute the exchanged messages (35). Additionally, the presence of an individual DNN module implies that relatively large amounts of data are required in order to train it. Nonetheless, the fact that this DNN only produces a correction term which is interleaved with the model-based algorithm operation implies that the amount of training data required to achieve a given accuracy is notably smaller compared to that required when using solely the DNN for inference. For instance, the quantitative example of the neural augmented Kalman smoother demonstrate that it requires 10 – 20 times less samples compared to that required by the individual GNN to achieve similar MSE results.

In summary, the main benefits of neural augmentation over purely model-based inference thus lie in its ability to improve and robustify performance in the presence of inaccurate domain knowledge. Compared to inferring solely based on deep learning, neural augmentation enables to train with smaller data sets, or alternatively, to infer at improved accuracy for a given limited data set, due to its interaction with the model-based component.

VI. CONCLUSIONS AND FUTURE CHALLENGES

In this article, we presented a mapping of methods for combining domain knowledge and data-driven inference via model-based deep learning in a tutorial manner. In particular, we noted that hybrid model-based/data-driven systems can be categorized into model-aided networks, which utilize model-based algorithms to design DNN architectures, and DNN-aided inference, where deep learning is integrated into traditional model-based methods. We detailed leading design approaches for each strategy in a systematic manner, along with design guidelines and concrete examples. To conclude this overview, we first summarize the key advantages of model-based deep learning in Subsection VI-A. Then, we present guidelines for selecting a design approach for a given application in Subsection VI-B, intended to facilitate the derivation of future hybrid data-driven/model-based systems. Finally, we review some future research challenges in Subsection VI-C.

A. Advantages of Model-Based Deep Learning

The combination of traditional handcrafted algorithms with emerging data-driven tools via model-based deep learning brings forth several key advantages. Compared to purely model-based schemes, the integration of data-driven deep learning facilitates inference in complex environments, where accurately capturing the underlying model in a closed-form mathematical expression may be infeasible. For instance, incorporating DNN-based implicit regularization was shown to enable CS beyond its traditional domain of sparse signals, as discussed in Subsection V-A, while the implementation of the SIC method as an interconnection of neural building blocks enables its operation in non-linear setups, as demonstrated in Subsection IV-B. The model-agnostic nature of deep learning also allows hybrid model-based/data-driven inference to achieve improved resiliency to model uncertainty compared to inferring solely based on domain knowledge, as the combination of DNNs allows the resulting system to learn to overcome such uncertainty from data. For example, empowering model-based Kalman smoothing by neural augmentation was shown in Subsection V-C to notably improve its performance when the state-space model does not fully reflect the true dynamics, while the usage of learned factor graphs for SP inference was demonstrated to result in improved robustness to model uncertainty in Subsection V-B. Finally, the fact that hybrid systems learn to carry out part of their inference based on data may allow model-based deep learning methods to operate with reduced delay compared to the corresponding fully model-based methods, as demonstrated by deep unfolding in Subsection IV-A.

Compared to utilizing conventional DNN architectures for inference, the incorporation of domain knowledge via a hybrid model-based/data-driven design results in systems which are tailored for the problem at hand. As a result, model-based deep learning systems require notably less data in order to learn an accurate mapping, as demonstrated in the comparison of learned factor graphs and the sliding bidirectional RNN system in the quantitative example in Subsection V-B, as well as the comparison between the neural augmented Kalman smoother and the GNN state estimator in the corresponding example in Subsection V-C. This property of model-based deep learning systems enables quick adaptation to variations in the underlying statistical model, as shown in [16]. Finally, a system combining DNNs with model-based inference often provides the ability to analyze its resulting predictions, yielding interpretability and confidence which are commonly challenging to obtain with conventional black-box deep learning.

B. Choosing a Model-Based Deep Learning Strategy

The aforementioned gains of model-based deep learning are shared at some level by all the different approaches presented in Sections IV-V. However, each strategy is focused on exploiting a different advantage of hybrid model-based/data-driven inference, particularly in the context of signal processing oriented applications. Consequently, to complement the mapping of model-based deep learning strategies and facilitate the implementation of future application-specific hybrid systems, we next enlist the main considerations one should take

into account when seeking to combine model-based methods with data-driven tools for a given problem of interest.

Step 1: Domain knowledge and data characterization:

First, one must ensure the availability of the two key ingredients in model-based deep learning, i.e., domain knowledge and data. The former corresponds to what is known *a priori* about the problem at hand, in terms of statistical models and established assumptions, as well as what is unknown, or is based on some approximation of the environment which is likely to be inaccurate. The latter addresses the amount of labeled and unlabeled samples one possesses in advance for the considered problem, as well as whether or not they reflect the scenario in which the system is requested to infer in practice.

Step 2: Identifying a model-based method: Based on the available domain knowledge, the next step is to identify a suitable model-based algorithm for the problem. This choice should rely on the portion of the domain knowledge which is *available*, and not on what is *unknown*, as the latter can be compensated for by integration of deep learning tools. This stage must also consider the requirements of the inference system in terms of performance, complexity, and real-time operation, as these are encapsulated in the selection of the algorithm. The identification of a model-based algorithm, combined with the availability of domain knowledge and data, should also indicate whether model-based deep learning mechanisms are required for the application of interest.

Step 3: Implementation challenges: Having identified a suitable model-based algorithm for the specific application, the selection of the approach to combine it with deep learning should be based on the understanding of its main implementation challenges. Some representative implementation issues and their relationship with the recommended model-based deep learning approaches include:

- 1) Missing domain knowledge - model-based deep learning can implement the model-based inference algorithm when parts of the underlying model are unknown, or alternatively, too complex to be captured analytically, by harnessing the model-agnostic nature of deep learning. In this case, the selection of the implementation approach depends on the format of the identified model-based algorithm: When it builds upon some known structures via, e.g., message passing based inference, structure-oriented DNN-aided inference detailed in Subsection V-B can be most suitable as means of integrating DNNs to enable operation with missing domain knowledge. Similarly, when the missing domain knowledge can be represented as some complex search domain, or alternatively, an unknown and possibly intractable regularization term, structure-agnostic DNN-aided inference detailed in Subsection V-A can typically facilitate optimization with implicitly learned regularizers. Finally, when the algorithm can be represented as an interconnection of model-dependent building blocks, one can maintain the overall flow of the algorithm while operating in a model-agnostic manner via neural building blocks, as discussed in Subsection IV-B.
- 2) Inaccurate domain knowledge - model-based algorithms are typically sensitive to inaccurate knowledge of the

underlying model and its parameters. In such cases, where one has access to a complete description of the underlying model up to some uncertainty, model-based deep learning can robustify the model-based algorithm and learn to achieve improved accuracy. A candidate approach to robustify model-based processing is by adding a learned correction term via neural augmentation, as detailed in Subsection V-C. Alternatively, when the model-based algorithm takes an iterative form, improved resiliency can be obtained by unfolding the algorithm into a DNN, as discussed in Subsection IV-A.

- 3) Inference speed - model-based deep learning can learn to implement iterative inference algorithms, which typically require a large amount of iterations to converge, with reduced inference speed. This is achieved by designing model-aided networks, either via deep unfolding (see Subsection IV-A) or neural building blocks (see Subsection IV-B). The fact that model-aided networks learn their iterative computations from data allows the resulting system to infer reliably with a much smaller number of iteration-equivalent layers, compared to the iterations required by the model-based algorithm.

The aforementioned implementation challenges constitute only a partial list of the considerations one should account for when selecting a model-based deep learning design approach. Additional considerations include computational capabilities during both training as well as inference; the need to handle variations in the statistical model, which in turn translate to a possible requirement to periodically re-train the system; and the quantity and the type of available data. Nonetheless, the division of the steps above provide systematic guidelines which one can utilize and possibly extend when seeking to implement an inference system while having some access to both data and domain knowledge. Finally, we note that some of the detailed model-based deep learning strategies can be combined, and thus one can select more than a single design approach. For instance, one can interleave DNN-aided inference via implicitly learned regularization and/or priors, with deep unfolding of the iterative optimization algorithm, as discussed in Subsection V-A.

C. Future Research Directions

We end by discussing a few representative unexplored research aspects of model-based deep learning:

Performance Guarantees: One of the key strengths of model-based algorithms is their established theoretical performance guarantees. In particular, the analytical tractability of model-based methods implies that one can quantify their expected performance as a function of the parameters of underlying statistical or deterministic models. For conventional deep learning, such performance guarantees are very challenging to characterize, and deeper theoretical understanding is a crucial missing component. The combination of deep learning with model-based structure increases interpretability thus possibly leading to theoretical guarantees. Theoretical guarantees improve the reliability of hybrid model-based/data-driven systems, as well as improve performance. For example, some preliminary theoretical results were identified for specific

model-based deep learning methods, such as the convergence analysis of plug-and-play networks for regularized optimization in [63].

Deep Learning Algorithms: Improving model interpretability and incorporating human knowledge is crucial for artificial intelligence development. Model-based deep learning can constitute a systematic framework to incorporate domain knowledge into data-driven systems, and can thus give rise to new forms of deep learning algorithms, such as interpretable DNN architectures which follow traditional model-based methods to account for domain knowledge.

Collaborative Model-Based Deep Learning: The increasing demands for accessible and personalized artificial intelligence give rise to the need to operate DNNs on edge devices such as smartphones, sensors, and autonomous cars [6]. The limited computational and data resources of edge devices make model-based deep learning strategies particularly attractive for edge intelligence. Privacy constraints for mobile and sensitive data are further driving research in distributed training e.g. through the framework of federated learning [88], [89]. Combining model-based structures with federated learning and distributed model-based inference remains as interesting research directions.

Unexplored Applications: The increasing interest in hybrid model-based/data-driven deep learning methods is motivated by the need for robustness and structural understanding. Applications falling under the broad family of signal processing, communications, and control problems are natural candidates to benefit due to the proliferation of established model-based algorithms. We believe that model-based deep learning can contribute to the development of emerging technologies such as IOT networks, autonomous systems and wireless communications.

REFERENCES

- [1] Y. LeCun, Y. Bengio, and G. Hinton, "Deep learning," *Nature*, vol. 521, no. 7553, p. 436, 2015.
- [2] K. He, X. Zhang, S. Ren, and J. Sun, "Delving deep into rectifiers: Surpassing human-level performance on imagenet classification," in *Proceedings of the IEEE international conference on computer vision*, 2015, pp. 1026–1034.
- [3] D. Silver, J. Schrittwieser, K. Simonyan, I. Antonoglou, A. Huang, A. Guez, T. Hubert, L. Baker, M. Lai, A. Bolton, Y. Chen, T. Lillicrap, F. Hui, L. Sifre, G. van den Driessche, T. Graepel, and D. Hassabis, "Mastering the game of go without human knowledge," *Nature*, vol. 550, no. 7676, pp. 354–359, 2017.
- [4] O. Vinyals, I. Babuschkin, W. M. Czarnecki, M. Mathieu, A. Dudzik, J. Chung, D. H. Choi, R. Powell, T. Ewalds, P. Georgiev, J. Oh, D. Horgan, M. Kroiss, I. Danihelka, A. Huang, L. Sifre, T. Cai, J. P. Agapiou, M. Jaderberg, A. S. Vezhnevets, R. Leblond, T. Pohlen, V. Dalibard, D. Budden, Y. Sulsky, J. Molloy, T. L. Paine, C. Gulcehre, Z. Wang, T. Pfaff, Y. Wu, R. Ring, D. Yogatama, D. Wünsch, K. McKinney, O. Smith, T. Schaul, T. Lillicrap, K. Kavukcuoglu, D. Hassabis, C. Apps, and D. Silver, "Grandmaster level in StarCraft II using multi-agent reinforcement learning," *Nature*, vol. 575, no. 7782, pp. 350–354, 2019.
- [5] Y. Bengio, "Learning deep architectures for AI," *Foundations and Trends in Machine Learning*, vol. 2, no. 1, pp. 1–127, 2009.
- [6] J. Chen and X. Ran, "Deep learning with edge computing: A review," *Proc. IEEE*, 2019.
- [7] V. Monga, Y. Li, and Y. C. Eldar, "Algorithm unrolling: Interpretable, efficient deep learning for signal and image processing," *arXiv preprint arXiv:1912.10557*, 2019.
- [8] K. Gregor and Y. LeCun, "Learning fast approximations of sparse coding," in *Proceedings of the 27th International Conference on International Conference on Machine Learning*, 2010, pp. 399–406.
- [9] S. Wu, A. Dimakis, S. Sanghavi, F. Yu, D. Holtmann-Rice, D. Storchescu, A. Rostamizadeh, and S. Kumar, "Learning a compressed sensing measurement matrix via gradient unrolling," in *International Conference on Machine Learning*, 2019, pp. 6828–6839.
- [10] A. Bora, A. Jalal, E. Price, and A. G. Dimakis, "Compressed sensing using generative models," in *Proceedings of the 34th International Conference on Machine Learning-Volume 70*. JMLR. org, 2017, pp. 537–546.
- [11] D. Van Veen, A. Jalal, M. Soltanolkotabi, E. Price, S. Vishwanath, and A. G. Dimakis, "Compressed sensing with deep image prior and learned regularization," *arXiv preprint arXiv:1806.06438*, 2018.
- [12] J. Whang, Q. Lei, and A. G. Dimakis, "Compressed sensing with invertible generative models and dependent noise," *arXiv preprint arXiv:2003.08089*, 2020.
- [13] D. Gilton, G. Ongie, and R. Willett, "Neumann networks for inverse problems in imaging," *arXiv preprint arXiv:1901.03707*, 2019.
- [14] S. V. Venkatakrishnan, C. A. Bouman, and B. Wohlberg, "Plug-and-play priors for model based reconstruction," in *Global Conference on Signal and Information Processing (GlobalSIP)*. IEEE, 2013, pp. 945–948.
- [15] H. K. Aggarwal, M. P. Mani, and M. Jacob, "MoDL: Model-based deep learning architecture for inverse problems," *IEEE Trans. Med. Imag.*, vol. 38, no. 2, pp. 394–405, 2018.
- [16] N. Shlezinger, N. Farsad, Y. C. Eldar, and A. J. Goldsmith, "ViterbiNet: A deep learning based Viterbi algorithm for symbol detection," *IEEE Trans. Wireless Commun.*, vol. 19, no. 5, pp. 3319–3331, 2020.
- [17] N. Shlezinger, R. Fu, and Y. C. Eldar, "DeepSIC: Deep soft interference cancellation for multiuser MIMO detection," *IEEE Trans. Wireless Commun.*, 2020.
- [18] N. Farsad, N. Shlezinger, A. J. Goldsmith, and Y. C. Eldar, "Data-driven symbol detection via model-based machine learning," *arXiv preprint arXiv:2002.07806*, 2020.
- [19] N. Samuel, T. Diskin, and A. Wiesel, "Learning to detect," *IEEE Trans. Signal Process.*, vol. 67, no. 10, pp. 2554–2564, 2019.
- [20] K. Pratik, B. D. Rao, and M. Welling, "RE-MIMO: Recurrent and permutation equivariant neural MIMO detection," *arXiv preprint arXiv:2007.00140*, 2020.
- [21] V. G. Satorras and M. Welling, "Neural enhanced belief propagation on factor graphs," *arXiv preprint arXiv:2003.01998*, 2020.
- [22] G. Ongie, A. Jalal, C. A. Metzler, R. G. Baraniuk, A. G. Dimakis, and R. Willett, "Deep learning techniques for inverse problems in imaging," *IEEE Journal on Selected Areas in Information Theory*, vol. 1, no. 1, pp. 39–56, 2020.
- [23] J. R. Hershey, J. L. Roux, and F. Weninger, "Deep unfolding: Model-based inspiration of novel deep architectures," *arXiv preprint arXiv:1409.2574*, 2014.
- [24] M. Kocaoglu, C. Snyder, A. G. Dimakis, and S. Vishwanath, "Causal-GAN: Learning causal implicit generative models with adversarial training," *arXiv preprint arXiv:1709.02023*, 2017.
- [25] C. Metzler, A. Mousavi, and R. Baraniuk, "Learned D-AMP: Principled neural network based compressive image recovery," in *Advances in Neural Information Processing Systems*, 2017, pp. 1772–1783.
- [26] Y. C. Eldar and G. Kutyniok, *Compressed sensing: theory and applications*. Cambridge university press, 2012.
- [27] Y. C. Eldar, *Sampling theory: Beyond bandlimited systems*. Cambridge University Press, 2015.
- [28] I. Goodfellow, Y. Bengio, and A. Courville, *Deep learning*. MIT press, 2016.
- [29] S. Hochreiter and J. Schmidhuber, "Long short-term memory," *Neural computation*, vol. 9, no. 8, pp. 1735–1780, 1997.
- [30] A. Vaswani, N. Shazeer, N. Parmar, J. Uszkoreit, L. Jones, A. N. Gomez, Ł. Kaiser, and I. Polosukhin, "Attention is all you need," in *Advances in neural information processing systems*, 2017, pp. 5998–6008.
- [31] Y. LeCun and Y. Bengio, "Convolutional networks for images, speech, and time series," *The handbook of brain theory and neural networks*, vol. 3361, no. 10, p. 1995, 1995.
- [32] T. Tieleman and G. Hinton, "Lecture 6.5-RMSProp: Divide the gradient by a running average of its recent magnitude," *COURSERA: Neural networks for machine learning*, vol. 4, no. 2, pp. 26–31, 2012.
- [33] D. P. Kingma and J. Ba, "Adam: A method for stochastic optimization," *arXiv preprint arXiv:1412.6980*, 2014.
- [34] A. Krizhevsky, I. Sutskever, and G. E. Hinton, "Imagenet classification with deep convolutional neural networks," *Communications of the ACM*, vol. 60, no. 6, pp. 84–90, 2017.
- [35] I. Goodfellow, J. Pouget-Abadie, M. Mirza, B. Xu, D. Warde-Farley, S. Ozair, A. Courville, and Y. Bengio, "Generative adversarial nets," in *Advances in neural information processing systems*, 2014, pp. 2672–2680.

- [36] T. Karras, S. Laine, M. Aittala, J. Hellsten, J. Lehtinen, and T. Aila, "Analyzing and improving the image quality of stylegan," in *Proceedings of the IEEE/CVF Conference on Computer Vision and Pattern Recognition*, 2020, pp. 8110–8119.
- [37] P. Vincent, H. Larochelle, Y. Bengio, and P.-A. Manzagol, "Extracting and composing robust features with denoising autoencoders," in *Proceedings of the 25th international conference on Machine learning*, 2008, pp. 1096–1103.
- [38] D. P. Kingma and M. Welling, "Auto-encoding variational bayes," *arXiv preprint arXiv:1312.6114*, 2013.
- [39] Y. Li, M. Tofighi, J. Geng, V. Monga, and Y. C. Eldar, "Deep algorithm unrolling for blind image deblurring," *arXiv preprint arXiv:1902.03493*, 2019.
- [40] O. Solomon, R. Cohen, Y. Zhang, Y. Yang, Q. He, J. Luo, R. J. van Sloun, and Y. C. Eldar, "Deep unfolded robust PCA with application to clutter suppression in ultrasound," *IEEE Trans. Med. Imag.*, 2019.
- [41] Y. Cui, S. Li, and W. Zhang, "Jointly sparse signal recovery and support recovery via deep learning with applications in MIMO-based grant-free random access," *IEEE J. Sel. Areas Commun.*, 2020.
- [42] T. Chang, B. Tolooshams, and D. Ba, "RandNet: deep learning with compressed measurements of images," in *Proc. IEEE MLSP*, 2019.
- [43] B. Tolooshams, A. H. Song, S. Temereanca, and D. Ba, "Convolutional dictionary learning based auto-encoders for natural exponential-family distributions," *arXiv preprint arXiv:1908.09258*, 2019.
- [44] A. Balatsoukas-Stimming and C. Studer, "Deep unfolding for communications systems: A survey and some new directions," *arXiv preprint arXiv:1906.05774*, 2019.
- [45] H. He, C.-K. Wen, S. Jin, and G. Y. Li, "Model-driven deep learning for MIMO detection," *IEEE Trans. Signal Process.*, vol. 68, pp. 1702–1715, 2020.
- [46] S. Takabe, M. Imanishi, T. Wadayama, R. Hayakawa, and K. Hayashi, "Trainable projected gradient detector for massive overloaded MIMO channels: Data-driven tuning approach," *IEEE Access*, vol. 7, pp. 93 326–93 338, 2019.
- [47] Q. Hu, Y. Cai, Q. Shi, K. Xu, G. Yu, and Z. Ding, "Iterative algorithm induced deep-unfolding neural networks: Precoding design for multiuser MIMO systems," *IEEE Trans. Wireless Commun.*, 2020.
- [48] R. J. van Sloun, R. Cohen, and Y. C. Eldar, "Deep learning in ultrasound imaging," *Proc. IEEE*, vol. 108, no. 1, pp. 11–29, 2019.
- [49] M. Mischi, M. A. L. Bell, R. J. van Sloun, and Y. C. Eldar, "Deep learning in medical ultrasound—from image formation to image analysis," *IEEE Trans. Ultrason., Ferroelectr., Freq. Control*, vol. 67, no. 12, pp. 2477–2480, 2020.
- [50] G. Dardikman-Yoffe and Y. C. Eldar, "Learned SPARCOM: Unfolded deep super-resolution microscopy," *Optics Express*, vol. 28, no. 19, pp. 4797–4812, 2020.
- [51] K. Zhang, L. V. Gool, and R. Timofte, "Deep unfolding network for image super-resolution," in *Proceedings of the IEEE/CVF Conference on Computer Vision and Pattern Recognition*, 2020, pp. 3217–3226.
- [52] Y. Huang, S. Li, L. Wang, and T. Tan, "Unfolding the alternating optimization for blind super resolution," *Advances in Neural Information Processing Systems*, vol. 33, 2020.
- [53] R. Otazo, E. Candes, and D. K. Sodickson, "Low-rank plus sparse matrix decomposition for accelerated dynamic MRI with separation of background and dynamic components," *Magnetic resonance in medicine*, vol. 73, no. 3, pp. 1125–1136, 2015.
- [54] A. Beck and M. Teboulle, "A fast iterative shrinkage-thresholding algorithm for linear inverse problems," *SIAM journal on imaging sciences*, vol. 2, no. 1, pp. 183–202, 2009.
- [55] D. P. Palomar and Y. C. Eldar, *Convex optimization in signal processing and communications*. Cambridge university press, 2010.
- [56] Y. Li, M. Tofighi, J. Geng, V. Monga, and Y. C. Eldar, "An algorithm unrolling approach to deep blind image deblurring," *arXiv preprint arXiv:1902.03493*, 2019.
- [57] J. Duan, J. Schlemper, C. Qin, C. Ouyang, W. Bai, C. Biffi, G. Bello, B. Statton, D. P. O'Regan, and D. Rueckert, "VS-Net: Variable splitting network for accelerated parallel mri reconstruction," in *International Conference on Medical Image Computing and Computer-Assisted Intervention*. Springer, 2019, pp. 713–722.
- [58] W.-J. Choi, K.-W. Cheong, and J. M. Cioffi, "Iterative soft interference cancellation for multiple antenna systems," in *Proc. WCNC*, 2000, pp. 304–309.
- [59] S. Boyd, N. Parikh, and E. Chu, *Distributed optimization and statistical learning via the alternating direction method of multipliers*. Now Publishers Inc, 2011.
- [60] A. Chambolle and T. Pock, "A first-order primal-dual algorithm for convex problems with applications to imaging," *Journal of mathematical imaging and vision*, vol. 40, no. 1, pp. 120–145, 2011.
- [61] R. Ahmad, C. A. Bouman, G. T. Buzzard, S. Chan, S. Liu, E. T. Reehorst, and P. Schniter, "Plug-and-play methods for magnetic resonance imaging: Using denoisers for image recovery," *IEEE Signal Process. Mag.*, vol. 37, no. 1, pp. 105–116, 2020.
- [62] K. Zhang, W. Zuo, S. Gu, and L. Zhang, "Learning deep CNN denoiser prior for image restoration," in *Proceedings of the IEEE conference on computer vision and pattern recognition*, 2017, pp. 3929–3938.
- [63] E. K. Ryu, J. Liu, S. Wang, X. Chen, Z. Wang, and W. Yin, "Plug-and-play methods provably converge with properly trained denoisers," *arXiv preprint arXiv:1905.05406*, 2019.
- [64] S. Ono, "Primal-dual plug-and-play image restoration," *IEEE Signal Process. Lett.*, vol. 24, no. 8, pp. 1108–1112, 2017.
- [65] U. S. Kamilov, H. Mansour, and B. Wohlberg, "A plug-and-play priors approach for solving nonlinear imaging inverse problems," *IEEE Signal Process. Lett.*, vol. 24, no. 12, pp. 1872–1876, 2017.
- [66] T. Meinhardt, M. Moller, C. Hazirbas, and D. Cremers, "Learning proximal operators: Using denoising networks for regularizing inverse imaging problems," in *Proceedings of the IEEE International Conference on Computer Vision*, 2017, pp. 1781–1790.
- [67] E. J. Candès, J. Romberg, and T. Tao, "Robust uncertainty principles: Exact signal reconstruction from highly incomplete frequency information," *IEEE Trans. Inf. Theory*, vol. 52, no. 2, pp. 489–509, 2006.
- [68] D. L. Donoho, "Compressed sensing," *IEEE Trans. Inf. Theory*, vol. 52, no. 4, pp. 1289–1306, 2006.
- [69] A. Radford, L. Metz, and S. Chintala, "Unsupervised representation learning with deep convolutional generative adversarial networks," *arXiv preprint arXiv:1511.06434*, 2015.
- [70] Z. Liu, P. Luo, X. Wang, and X. Tang, "Deep learning face attributes in the wild," in *Proceedings of International Conference on Computer Vision (ICCV)*, December 2015.
- [71] Y. LeCun and C. Cortes, "MNIST handwritten digit database," 2010. [Online]. Available: <http://yann.lecun.com/exdb/mnist/>
- [72] K. Zhang, W. Zuo, Y. Chen, D. Meng, and L. Zhang, "Beyond a Gaussian denoiser: Residual learning of deep CNN for image denoising," *IEEE Trans. Image Process.*, vol. 26, no. 7, pp. 3142–3155, 2017.
- [73] S. Diamond, V. Sitzmann, F. Heide, and G. Wetzstein, "Unrolled optimization with deep priors," *arXiv preprint arXiv:1705.08041*, 2017.
- [74] N. Shlezinger, N. Farsad, Y. C. Eldar, and A. J. Goldsmith, "Data-driven factor graphs for deep symbol detection," *arXiv preprint arXiv:2002.00758*, 2020.
- [75] A. Arnab, S. Zheng, S. Jayasumana, B. Romera-Paredes, M. Larsson, A. Kirillov, B. Savchynskyy, C. Rother, F. Kahl, and P. H. Torr, "Conditional random fields meet deep neural networks for semantic segmentation: Combining probabilistic graphical models with deep learning for structured prediction," *IEEE Signal Process. Mag.*, vol. 35, no. 1, pp. 37–52, 2018.
- [76] S. Chandra and I. Kokkinos, "Fast, exact and multi-scale inference for semantic image segmentation with deep Gaussian CRFs," in *European conference on computer vision*. Springer, 2016, pp. 402–418.
- [77] P. Knobelreiter, C. Sormann, A. Shekhovtsov, F. Fraundorfer, and T. Pock, "Belief propagation reloaded: Learning BP-layers for labeling problems," in *Proceedings of the IEEE/CVF Conference on Computer Vision and Pattern Recognition*, 2020, pp. 7900–7909.
- [78] B. Luijten, R. Cohen, F. J. De Bruijn, H. A. Schmeitz, M. Mischi, Y. C. Eldar, and R. J. Van Sloun, "Adaptive ultrasound beamforming using deep learning," *IEEE Trans. Med. Imag.*, 2020.
- [79] H. Palangi, R. Ward, and L. Deng, "Distributed compressive sensing: A deep learning approach," *IEEE Trans. Signal Process.*, vol. 64, no. 17, pp. 4504–4518, 2016.
- [80] S. S. Haykin, *Adaptive filter theory*. Pearson Education India, 2005.
- [81] A. Viterbi, "Error bounds for convolutional codes and an asymptotically optimum decoding algorithm," *IEEE Trans. Inf. Theory*, vol. 13, no. 2, pp. 260–269, 1967.
- [82] N. Shlezinger, N. Farsad, Y. C. Eldar, and A. J. Goldsmith, "Inference from stationary time sequences via learned factor graphs," *arXiv preprint arXiv:2006.03258*, 2020.
- [83] F. R. Kschischang, B. J. Frey, and H.-A. Loeliger, "Factor graphs and the sum-product algorithm," *IEEE Trans. Inf. Theory*, vol. 47, no. 2, pp. 498–519, 2001.
- [84] H.-A. Loeliger, "An introduction to factor graphs," *IEEE Signal Process. Mag.*, vol. 21, no. 1, pp. 28–41, 2004.
- [85] N. Farsad and A. Goldsmith, "Neural network detection of data sequences in communication systems," *IEEE Trans. Signal Process.*, vol. 66, no. 21, pp. 5663–5678, 2018.

- [86] V. G. Satorras, Z. Akata, and M. Welling, "Combining generative and discriminative models for hybrid inference," in *Advances in Neural Information Processing Systems*, 2019, pp. 13 802–13 812.
- [87] K. Yoon, R. Liao, Y. Xiong, L. Zhang, E. Fetaya, R. Urtasun, R. Zemel, and X. Pitkow, "Inference in probabilistic graphical models by graph neural networks," in *2019 53rd Asilomar Conference on Signals, Systems, and Computers*. IEEE, 2019, pp. 868–875.
- [88] V. Smith, C.-K. Chiang, M. Sanjabi, and A. S. Talwalkar, "Federated multi-task learning," in *Advances in Neural Information Processing Systems*, 2017, pp. 4424–4434.
- [89] T. Li, A. K. Sahu, A. Talwalkar, and V. Smith, "Federated learning: Challenges, methods, and future directions," *IEEE Signal Processing Magazine*, vol. 37, no. 3, pp. 50–60, 2020.